Like CRP, PTX3 belongs to the pentraxin family and it is considered a surrogate marker of disease activity at sites of inflammation. Although PTX3 and CRP are weakly and positively related without significance, both markers reciprocally change in individuals who are obese or have MetS. Although HDL-C stimulation of the *PTX3* gene or PTX3 inhibition of the plasma complement pathway might account for the paradoxical change in PTX3, further study is needed for clarification. In conclusion, the plasma profiles of PTX3 and CRP in 226 nonmedicated males indicated that these proteins inversely participate in the development of obesity or MetS.

ACKNOWLEDGMENTS

This study was supported by the Program of Fundamental Studies in Health Sciences of the NIBIO, NEDO, and by the Fund for Science and Technology from the Ministry of Education, Culture, Sports, Science and Technology in Japan.

DISCLOSURE

M.S. was a full-time employee of Perseus Proteomics Inc. Other authors declared no conflict of interest.

REFERENCES

1. Castell JV, Gómez-Lechón MJ, David M *et al.* Acute-phase response of human hepatocytes: regulation of acute-phase protein synthesis by interleukin-6. *Hepatology* 1990;12:1179–1186.
2. Visser M, Bouter LM, McQuillan GM, Wener MH, Harris TB. Elevated C-reactive protein levels in overweight and obese adults. *JAMA* 1999;282:2131–2135.
3. Bottazzi B, Vouret-Craviari V, Bastone A *et al.* Multimer formation and ligand recognition by the long pentraxin PTX3. Similarities and differences with the short pentraxins C-reactive protein and serum amyloid P component. *J Biol Chem* 1997;272:32817–32823.
4. Lee GW, Lee TH, Vilcek J. TSG-14, a tumor necrosis factor- and IL-1-inducible protein, is a novel member of the pentaxin family of acute phase proteins. *J Immunol* 1993;150:1804–1812.
5. Klouche M, Peri G, Knabbe C *et al.* Modified atherogenic lipoproteins induce expression of pentraxin-3 by human vascular smooth muscle cells. *Atherosclerosis* 2004;175:221–228.
6. Jaillon S, Peri G, Delneste Y *et al.* The humoral pattern recognition receptor PTX3 is stored in neutrophil granules and localizes in extracellular traps. *J Exp Med* 2007;204:793–804.
7. Abderrahim-Ferkoune A, Bezy O, Chiellini C *et al.* Characterization of the long pentraxin PTX3 as a TNFα-induced secreted protein of adipose cells. *J Lipid Res* 2003;44:994–1000.
8. Tong M, Carrero JJ, Qureshi AR *et al.* Plasma pentraxin 3 in patients with chronic kidney disease: associations with renal function, protein-energy wasting, cardiovascular disease, and mortality. *Clin J Am Soc Nephrol* 2007;2:889–897.
9. Sulıman ME, Yilmaz MI, Carrero JJ *et al.* Novel links between the long pentraxin 3, endothelial dysfunction, and albuminuria in early and advanced chronic kidney disease. *Clin J Am Soc Nephrol* 2008;3:976–985.
10. Inoue K, Sugiyama A, Reid PC *et al.* Establishment of a high sensitivity plasma assay for human pentraxin3 as a marker for unstable angina pectoris. *Arterioscler Thromb Vasc Biol* 2007;27:161–167.
11. Peri G, Introna M, Corradi D *et al.* PTX3, A prototypical long pentraxin, is an early indicator of acute myocardial infarction in humans. *Circulation* 2000;102:636–641.
12. Alberti L, Gilardini L, Zulian A *et al.* Expression of long pentraxin PTX3 in human adipose tissue and its relation with cardiovascular risk factors. *Atherosclerosis* 2009;202:455–460.
13. Yamasaki K, Kurimura M, Kasai T *et al.* Determination of physiological plasma pentraxin-3 (PTX3) levels in healthy populations. *Clin Chem Lab Med* 2009;47:471–477.
14. Sulıman ME, Qureshi AR, Carrero JJ *et al.* The long pentraxin PTX-3 in prevalent hemodialysis patients: associations with comorbidities and mortality. *QJM* 2008;101:397–405.
15. Bosutti A, Malaponte G, Zanetti M *et al.* Calorie restriction modulates inactivity-induced changes in the inflammatory markers C-reactive protein and pentraxin-3. *J Clin Endocrinol Metab* 2008;93:3226–3229.
16. Norata GD, Marchesi P, Pirillo A *et al.* Long pentraxin 3, a key component of innate immunity, is modulated by high-density lipoproteins in endothelial cells. *Arterioscler Thromb Vasc Biol* 2008;28:925–931.
17. Furukawa S, Fujita T, Shimabukuro M *et al.* Increased oxidative stress in obesity and its impact on metabolic syndrome. *J Clin Invest* 2004;114:1752–1761.
18. Dias AA, Goodman AR, Dos Santos JL *et al.* TSG-14 transgenic mice have improved survival to endotoxemia and to CLP-induced sepsis. *J Leukoc Biol* 2001;69:928–936.
19. Salio M, Chimenti S, De Angelis N *et al.* Cardioprotective function of the long pentraxin PTX3 in acute myocardial infarction. *Circulation* 2008;117:1055–1064.
20. Nauta AJ, Bottazzi B, Mantovani A *et al.* Biochemical and functional characterization of the interaction between pentraxin 3 and C1q. *Eur J Immunol* 2003;33:465–473.

Microbiology and Immunology

Microbiol Immunol 2009; **53**: 573–581
doi:10.1111/j.1348-0421.2009.00159.x

ORIGINAL ARTICLE

Adrenomedullin treatment reduces intestinal inflammation and maintains epithelial barrier function in mice administered dextran sulphate sodium

Shinya Ashizuka[1], Kyoko Inagaki-Ohara[2,3], Kenji Kuwasako[4], Johji Kato[4], Haruhiko Inatsu[1] and Kazuo Kitamura[1]

[1]First Department of Internal Medicine, University of Miyazaki, Miyazaki, 889-1692, [2]Molecular Microbiology Group, Center of Molecular Biosciences (COMB), Tropical Biosphere Research Center, University of the Ryukyus, Okinawa, 903-0213, [3]Parasitic Disease Unit, Department of Infectious Disease, Faculty of Medicine, University of Miyazaki, Miyazaki, 889-1692, and [4]Frontier Science Research Center, University of Miyazaki, Miyazaki, 889-1692, Japan

ABSTRACT

Hyperactivation and hyperpermeability of the intestinal epithelium is a hallmark of IBD. AM has been shown to reduce the severity of colitis in the acetic acid and TNBS-induced colitis model, however the mechanism of the therapeutic effect of AM against the colitis has not been clarified. Here, we show that the protective capability of AM is associated with suppression of inflammation and maintenance of the intestinal epithelial barrier function. In the DSS-induced colitis model, intra-rectal AM-treated mice showed a reduction in loss of body weight and severity of colitis. AM-treatment suppressed phosphorylation of STAT1 and STAT3 in the colonic epithelium, and altered the cytokine balance in the intestinal T cells, with lower levels of IFN-γ and TNF-α but higher levels of TGF-β. Expression of the epithelial intercellular junctions such as tight and adherence junctions were sustained in the AM-treated mice. In contrast, the epithelial junctions were down-regulated in the control mice, leading to loss of epithelial barrier integrity and enhanced permeability. Collectively, these data indicate a broad spectrum of AM-induced effects with respect to protection against DSS-induced colitis, and suggest a potential therapeutic value of this treatment for IBD.

Key words adrenomedullin, colitis, epithelial barrier.

AM was originally isolated from human pheochromocytoma and identified as a vasodilatory peptide (1), and has since been shown to be constitutively produced by a variety of tissues such as gut and bronchial epithelium of humans (2, 3) and gut of mice and rats (4, 5). In addition, AM also exerts anti-inflammatory (6) and antimicrobial activity (7). Since the expression of AM and its receptor are up-regulated during inflammation (6, 8), AM has potential therapeutic value in inflammatory diseases as well as several other categories of disease such as hypertension, cardiovascular and renal disorders, cancer, and diabetes.

IBD, including CD and UC, is a chronic, relapsing, and remitting condition with unknown etiology which exhibits various features of dysregulated immunological

Correspondence
Kyoko Inagaki-Ohara, Molecular Microbiology Group, Center of Molecular Biosciences (COMB), Tropical Biosphere Research Center, University of the Ryukyus, Senbaru 1, Nishihara, Okinawa 903-0213, Japan.
Tel: 81 98 895 8968; fax: 81 98 895 8944; email: g079010@comb.u-ryukyu.ac.jp

Received 20 April 2009; revised 21 May 2009; accepted 9 June 2009.

List of Abbreviations: AM, adrenomedullin; AP, allophycocyanin; CD, Crohn's disease; DSS, dextran sulfate sodium; DTT, dithiothreitol; EC, epithelial cells; HE, hematoxylin and eosin; IBD, inflammatory bowel diseases; IEL, intestinal intraepithelial T lymphocytes; IFN-γ, interferon-γ; IL, Il-4, interleukin-4; JAK, Janus kinase; JAM, junctional adhesion molecule; mAb, monoclonal Ab; MHC, major histocompatibility complex; r, recombinant; STAT, signal transducer and activator of transcription; TCR, T cell receptor; TER, transepithelial electrical resistance; TGF-β, transforming growth factor-β; Th, T helper; TNBS, 2,4,6-trinitrobenzene sulfonic acid; TNF-γ, tumor necrosis factor-γ; UC, ulcerative colitis, ZO, zonula occludens.

systems (9, 10). The pathogenesis of IBD involves interplay of the genetic, microbial, and immune systems, resulting in chronic intestinal inflammation with disruption of epithelial integrity and barrier function and increased sensitivity to intestinal flora (11–14). Interaction between IEL and EC is necessary for maintenance of epithelial integrity and a physical barrier to prevent potential inflammatory responses and infectious challenges in the intestinal epithelium (14–19). Recently, we and others have reported that AM is a potent anti-inflammatory agent in rat acetic acid-induced colitis (20) and murine TNBS-induced colitis (21). However, the mechanisms of AM-mediated amelioration of colitis have not been clarified. In this study, we have investigated the effect of AM treatment on suppression of DSS-induced colitis in the context of maintenance of epithelial barrier function.

MATERIALS AND METHODS

Animals and peptide

Male C57BL/6 mice (7–9 weeks old) were purchased from Japan SLC (Hamamatsu, Japan), housed under specific pathogen-free conditions and maintained on standard pellet chow and water *ad libitum*. The recombinant (r) human AM used in this study was provided by Shionogi, (Osaka, Japan). All experiments were carried out in accordance with the regulations of the Animal Research Committee of the University of Miyazaki and University of the Ryukyus.

Treatment with AM and induction of colitis

AM (0.05 μg of AM diluted in 0.2 ml of saline) was delivered into the lumen of the colon via a 5 cm long animal feeding tube inserted into the rectum to a depth of approximately 3 cm from the anal verge. Non AM-treated (control) mice were administered 0.2 ml of saline without AM. AM and saline were administrated once a day for 7 days. To induce colitis, mice were given 1.8% DSS (molecular weight, 36 000–50 000 daltons; ICN Biomedicals, Aurora, Ohio, USA) in their drinking water for 7 days (from day 0 to 6). On day 7, their water was switched to regular drinking water.

Detection of anaerobes

Detection of anaerobes was performed as described previously (16).

Histological analysis

Paraffin-embedded colonic sections of 10% formalin-fixed tissues were stained with HE.

Disease evaluation

Intestinal inflammation in the mice was evaluated according to previously described criteria (22). The disease score was determined by a combination of ulceration (0, no ulceration; 1, presence of erosion; 2, presence of focal ulceration; 3, presence of multiple ulcerations) and histological scores (0–3, inflammatory cell infiltration; 0–3, epithelial cell elongation).

Preparation of EC, IEL and cell culture for cytokine ELISA

IEL and EC were isolated and prepared according to a previously published method (16). Briefly, dissected small segments of the intestines were incubated at 37°C for 40 min in an RPMI 1640 medium (Sigma-Aldrich, St. Louis, MO, USA) containing 10% FCS and 1 mM DTT with vigorous shaking. The tissue suspension was passed through a nylon mesh to remove debris and centrifuged through a 25/40/75% discontinuous Percoll (Sigma-Aldrich) gradient at 600 × g at 20°C for 20 min. The cells collected from the interface of 25/40% were EC, and that of 40/75% were IEL. IEL were cultured for 48 hr with anti-CD3 mAb in RPMI 1640 supplemented with 10% FCS. The supernatants were collected to estimate the cytokine contents by ELISA using mouse IFN-γ, IL-4, and TNF-α (e-Bioscience, San Diego, CA, USA) and TGF-β (Biosource International, Camarillo, CA, USA) according to the manufacturer's instructions.

Western blot analysis

Lysates were prepared from colonic EC and analyzed by Western blotting according to a published method (14). Abs used in the Western blotting were as follows: rabbit anti-PY-STAT3, anti-PY-STAT1, anti-STAT3 and anti-STAT1 (Cell Signaling Technology, Danvers, MA, USA), rabbit anti-ZO-1 and anti-occludin (Zymed, South San Francisco, CA, USA), mouse anti-E-cadherin (BD Transduction Laboratories, Lexington, KY, USA), mouse anti-β-catenin (BD Transduction Laboratories), and mouse anti-β-actin (Sigma, St Louis, MO, USA).

FACS analysis

IEL were stained with FITC-conjugated TCR$\gamma\delta$ (GL3), PE-conjugated TCRβ (H57–597), AP-conjugated CD3ε (145-2C11) mAb as described previously (16). Flow cytometry analysis was performed on a FACS calibur flow cytometer (Becton Dickinson, Franklin Lakes, NJ, USA). All mAbs were purchased from BD Pharmingen (San Jose, CA, USA).

RT-PCR and real-time PCR

Total RNA was extracted from freshly isolated EC using an RNeasy Mini kit (Qiagen, Valencia, CA, USA) and primed with 20 pmol of a random primer in mixtures for reverse transcription. The synthesized cDNA was amplified by PCR using primers specific for the murine junctional molecules. The primer sets for detection of these junctional molecules have previously been described (23). For quantitative analysis of mRNA, the synthesized cDNA was amplified by using primers and probes specific for ZO-1, occludin and β-actin cDNA sequences (TaqMan gene Expression Assays; Applied Biosystems, Foster, CA, USA) according to the manufacturer's instructions. Quantitative real-time PCR was performed by using an ABI Prism 7000 Sequence Detector System (Applied Biosystems Foster, CA, USA). Results are expressed as the n-fold difference relative to the expression of β-actin.

Measurement of TER

The functional integrity of tight junctions in cell layers established on filter inserts was assessed by measuring TER using a Millicel ERS Volt-ohm meter (Millipore, Bedford, MA, USA) as described previously (19). CMT93 cells, a murine intestinal epithelial cell line, were seeded on the apical chamber of a transwell using BD BioCoat Intestinal Epithelium Differentiation Environment (BD Biosciences Bedford, MA, USA) for 72 hr in a 5% CO_2 incubator according to the manufacturer's instructions, and developed a TER around 450 Ohm $\times$ cm^2. The culture medium was then removed from the apical and basolateral chambers and replaced with either fresh medium or medium containing 100 ng/ml rIFN-γ (Chemicon, Temecula, CA, USA) and AM (10^{-7}, 10^{-8} and 10^{-9} M). Values of TER are expressed as percentage of the initial resistance as follows:

% of initial resistance = ([resistance from each point]− [resistance from a blank]/[resistance from non-treated cells] − [resistance from a blank]) × 100. [1].

Statistical analysis

Data are presented as means ± SD. Statistical parameters were ascertained with Statview 4.51 software (Abacus Concepts, Berkeley, CA, USA). A P value of less than 0.05 was taken as significant.

RESULTS

AM administration abrogates colitis in DSS-treated mice

We investigated the therapeutic effect of intrarectally administered AM on the severity of DSS-induced colitis. Mice given DSS showed profound and sustained weight loss, a major symptom of colitis (Fig. 1a). In contrast, AM-treated mice exhibited maintenance of body weight and suppression of other clinical symptoms such as overt bleeding and diarrhea. The AM-treated mice remained healthy and experienced none of the long-term effects of colitis seen in the control mice by day 28, while all of the control mice succumbed (data not shown). These results indicate that the administration of AM significantly abrogates severe symptoms of DSS colitis.

Histological analysis revealed neutrophil and lymphocyte infiltration on day 3; furthermore, remarkable thickening of the colonic wall, excessive crypt abscesses, EC erosions, and destruction of epithelial integrity were observed in the control mice on day 10 after DSS administration (Fig. 1b). By contrast, the AM-treated mice exhibited lesions that were much less severe, although there was mild thickening of the colon wall. On day 14 after AM administration, no evidence of inflammation was observed in the AM-treated mice, whereas crypt hyperplasia and infiltrated inflammatory cells were still evident in the control mice. This finding was further supported by assessment of changes in disease score (Fig. 1c). These results indicate that treatment with AM reduces development of DSS-induced colitis and strikingly improves inflammatory symptoms.

In addition to anti-inflammatory activity, AM displays potent antimicrobial activity against a variety of Gram-negative and Gram-positive bacteria (7, 24). After induction of DSS colitis the number of anaerobes was significantly decreased in the AM-treated compared with the control mice (Fig. 2). Since increased numbers of facultative anaerobes can be associated with IBD in humans (13), these results suggest that AM protects against disruption of the mucosal epithelium through suppression and translocation of anaerobes into the intestinal mucosa, leading to recruitment and activation of immune cells.

AM administration decreases inflammatory cytokines and increases regulatory cytokines

Hyperactivation due to deregulation of cytokine signaling has been suggested as a cause of colitis in the murine model and in IBD patients (12). Th1-type cytokine and cytokines which belong to the IL-6 cytokine family have been reported to induce acute bowel inflammation in IBD patients (25, 26) and in DSS-treated mice (27). Suppression of colitis can also be attributed to cell-to-cell interaction between T cells and enterocytes causing changes in the cytokine profile (15, 16). The effect of AM-treatment was also seen at the level of cytokine production from

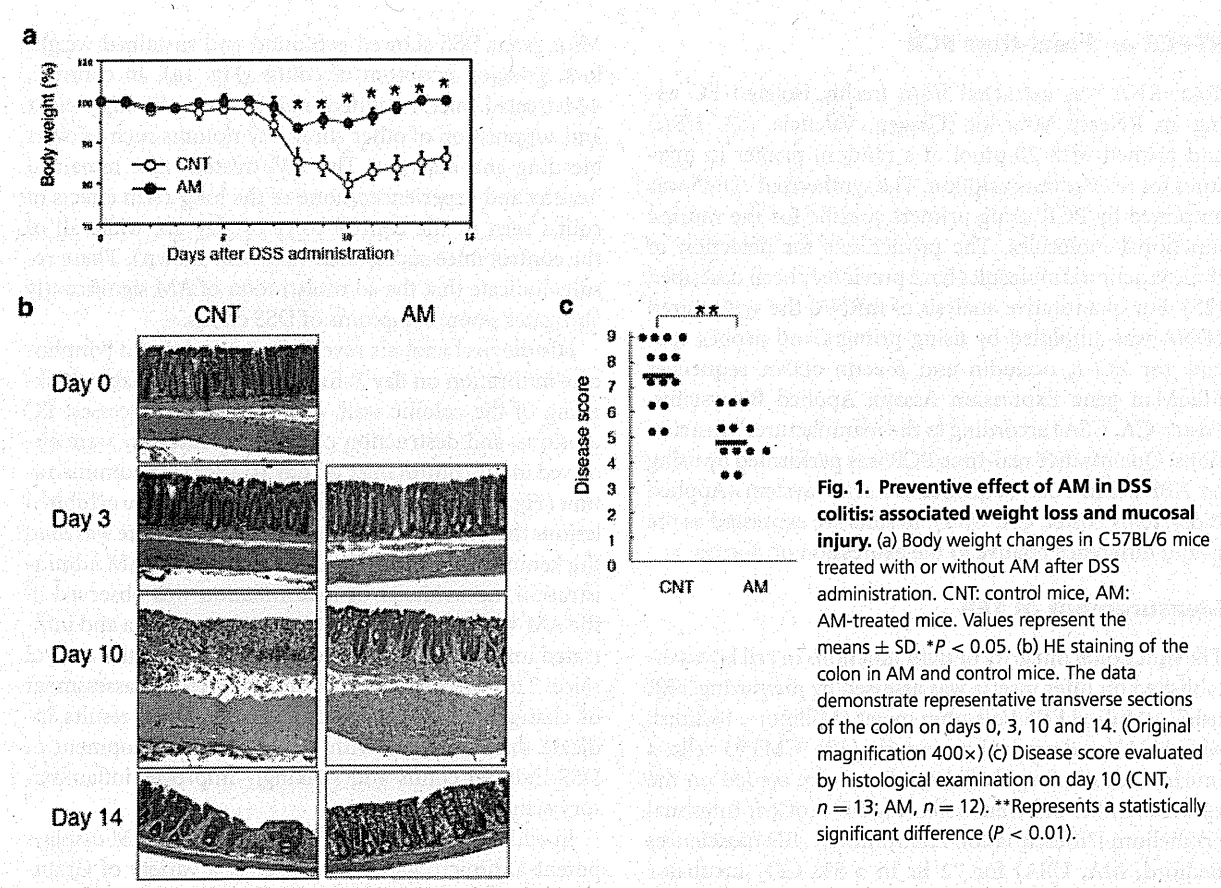

Fig. 1. Preventive effect of AM in DSS colitis: associated weight loss and mucosal injury. (a) Body weight changes in C57BL/6 mice treated with or without AM after DSS administration. CNT: control mice, AM: AM-treated mice. Values represent the means ± SD. $^*P < 0.05$. (b) HE staining of the colon in AM and control mice. The data demonstrate representative transverse sections of the colon on days 0, 3, 10 and 14. (Original magnification 400×) (c) Disease score evaluated by histological examination on day 10 (CNT, $n = 13$; AM, $n = 12$). **Represents a statistically significant difference ($P < 0.01$).

IEL of the large intestine. IEL isolated from the control mice consistently produced high concentrations of IFN-γ, TNF-α, and IL-6, with peak concentrations detected on day 10 after DSS administration (Fig. 3a). In contrast, AM treatment induced substantial TGF-β production, which did not occur in the IEL taken from the control mice. IL-4 production after DSS administration was not affected by AM treatment.

Cytokines bind to specific cell-surface receptors and activate cytoplasmic signal transduction pathways such as the JAK/STAT pathway (28). Continuous activation of STAT3 and STAT1 is often observed in patients with IBD as well as other inflammatory diseases (29, 30), and experimental and clinical data point toward aberrant activation of the Th1-dominant cytokine network. Since STAT3 is preferentially activated by IL-6 and its related cytokines and STAT1 is activated by IFN-γ (31), we examined both STAT3 and STAT1 activation. As shown in Figure 3b, in control mice STAT3 and STAT1 activation in the intestinal mucosa was observed on day 10; in contrast, their suppression was clearly shown in the AM-treated mice.

Since interaction between IEL and EC is important for the maintenance of intestinal homeostasis and both TCR$\alpha\beta^+$ and TCR$\gamma\delta^+$ T cells have been implicated in the development of colitis (16, 32, 33), we examined changes in the number of IEL and the proportion of TCR$\alpha\beta^+$ and TCR$\gamma\delta^+$ T cells in the IEL compartment of the large intestine. Although colonic CD3-positive IEL increased for 7 days following DSS administration in both control and AM-treated mice (Fig. 4a), TCR$\gamma\delta$ IEL decreased in the control mice, but not in the AM-treated mice (Fig. 4b). The number of IEL recovered to the initial amount in the AM-treated mice but not in the control mice. The induction of DSS colitis led to changes in the IEL profile, with a relative decrease in the TCR$\gamma\delta^+$ population on days 7 to 10 after DSS administration. Treatment of mice with AM prevented these alterations in the TCR$\alpha\beta$ and TCR$\gamma\delta$ IEL populations. Collectively, these results suggest that AM suppresses the production of proinflammatory cytokines by maintaining the TCR $\gamma\delta$ IEL and increasing the production of TGF-β expressed by the TCR $\gamma\delta$ IEL, thus leading to suppression of continuous STAT3 and STAT1 activation in EC.

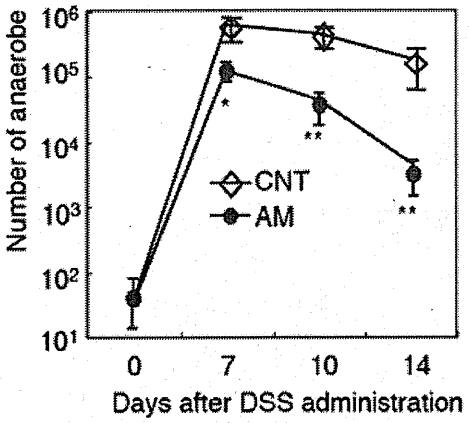

Fig. 2. The number of intestinal anaerobes in mice with DSS induced-colitis is decreased by AM treatment. Number of anaerobes was determined on day 7, 10 and 14 after AM administration. Three mice were used for each point. Values represent the means ± SD of three individual experiments. * and ** represent a statistically significant difference (*$P < 0.05$, **$P < 0.01$).

Treatment of mice with AM leads to recovery of junctional molecules in EC

To maintain the integrity of the intestinal epithelial barrier, EC express various junctional molecules including those associated with a tight junction; (ZO-1, occludin, and JAM); an adherens junction (β-catenin and E-cadherin); desmosomes (desmoglein-2) and a gap junction (connexin 26). The combined function of these molecules is to maintain the epithelial layer as a continuous impermeable belt to prevent paracellular crossing of a variety of luminal contents (34, 35). Expression of the junctional molecules is decreased in the course of colitis (23).

To evaluate the protective effect of AM against cytokine-induced impairment of the epithelial barrier *in vitro*, we examined TER by using CMT93 cells, a murine intestinal epithelial cell line. The TER of CMT93 cells was decreased by the addition of IFN-γ. The addition of AM increased the TER of the cells treated with IFN-γ in a dose-dependent manner (Fig. 5a). We next examined the degree of expression of specific mRNA for a variety of junctional molecules in large intestinal EC *in vivo*. Following induction of DSS-colitis, mRNA expression levels of junctional molecules in the tight junction, adherens junction, and desmosomes were drastically decreased on day 10 and had incompletely recovered on day 14 in the control mice (Fig. 5b). In contrast, these changes were much smaller in the AM-treated mice. There was a slight transient reduction in the expression of junctional molecule mRNA on day 10 of colitis induction, but full recovery was noted by day 14 in the AM-treated mice. Since ZO-1 and occludin are crucial for the formation of TER, we further examined their expression by real-time RT-PCR. ZO-1 expression in the control and AM-treated mice decreased and recovered in parallel. Occludin expression in the control mice continued to decrease, whereas that in the AM-treated mice was sustained (Fig. 5c). This result is coincident with the RT-PCR data shown in Figure 5a. Western blot data also showed decreased expression of junctional molecules in the control mice but maintenance of the initial degree of expression in the AM-treated mice, except in the case of ZO-1 (Fig. 5d). These results indicate that AM plays a role in maintaining the expression of junctional molecules and epithelial barrier function in the large intestine after induction of colitis.

DISCUSSION

Since IBD are refractory diseases of unknown etiology in humans, the development of new therapies is important. Recently, AM has been suggested as a candidate for IBD treatment because it acts as an anti-inflammatory agent in the rodent colitis model (20, 21). However, the mechanism of AM's protective effect against destruction of the epithelial barrier, which is a remarkable feature of IBD, has yet to be elucidated. This study is the first showing that the therapeutic effect of AM against colitis is correlated with maintenance of epithelial barrier integrity. The effects of AM on DSS-induced colitis include changes in cytokine production from IEL, and in expression of junctional molecules of EC and microbial flora, suggesting that AM exerts wide beneficial effects which protect against IBD.

The oral administration of DSS stimulates nonlymphoid cells such as EC and phagocytes, causing loss of body weight, mucosal ulcers, and neutrophil infiltration, and resulting in release of proinflammatory cytokines and destruction of the epithelial layer. Because DSS colitis occurs in mice lacking T cells, B cells, and NK cells, T cell-mediated immunity is not essential for induction of DSS colitis (36, 37). However, Th1-biased T cell-mediated immunity is activated in this model (38). We have clearly shown that AM suppresses Th1-type cytokines and subsequent proinflammatory responses associated with production of regulatory cytokines by IEL. These responses might be a mechanism for the therapeutic effect of AM treatment in colitis. Another therapeutic effect of AM based on a murine model of Crohn's disease has been reported: AM treatment was associated with down-regulation of both inflammatory and Th1-driven autoimmune responses, including regulation of a wide spectrum of inflammatory mediators mediated by $CD4^+CD25^+$ regulatory T cells (21). In the IBD models, colitis is ameliorated by TGF-β, an immunosuppressive

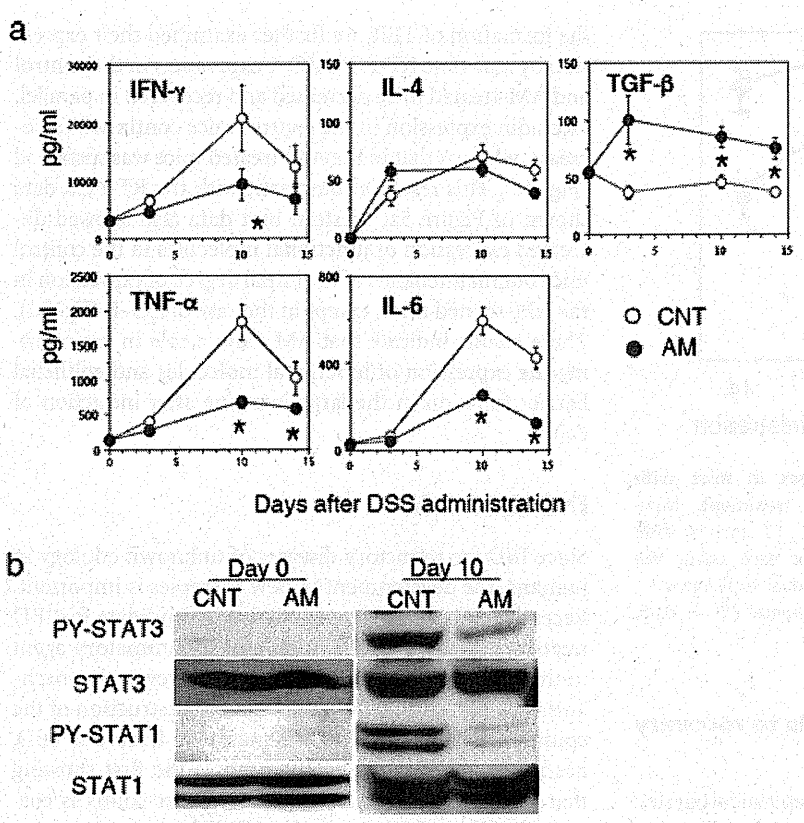

Fig. 3. AM administration suppresses the production of Th1- and inflammatory cytokines in the large intestine. (a) Changes in cytokine production of IEL. Three mice were used for each point. Values represent the means ± SD of three individual experiments. *Represents a statistically significant difference ($P < 0.05$). (b) Phosphorylation of STAT1 and STAT3 in colonic EC on days 0 and 10 after DSS administration.

cytokine produced by regulatory T cells (39, 40). TGF-β exerts a protective role against Th1-type colitis by suppressing the activated T cells (39, 41). Therefore, TGF-β produced by IEL of AM-treated mice also suppressed colitis in our experimental system.

TCR$\gamma\delta$ IEL can produce TGF-β and may suppress inflammation as regulatory T cells (42). In fact, C$\delta^{-/-}$ mice, which lack $\gamma\delta$ T cells, show a reduction in TGF-β production (16). In the present study, a decrease in TGF-β production by IEL may have been caused in part by a decrease in TCR$\gamma\delta$ IEL after DSS treatment of mice (Figs. 3a and 4). Because TCR$\gamma\delta$ IEL were maintained in AM-treated mice (Fig. 4b), the TCR$\gamma\delta$ IEL were assumed to be regulatory cells which suppress the Th1-type inflammatory response through cytokines or cell-to-cell interactions between EC and TCR$\alpha\beta$ IEL (15, 16). The IEL and EC reciprocally regulate their development and growth mediated by a variety of cytokines and their receptor signaling (15, 43, 44). C$\delta^{-/-}$ mice show a reduction in the turn-over of EC and down-regulation of expression of the MHC class II molecule (45). TCR$\gamma\delta$ IEL-mediated exertion of the suppressive function of EC may be an important mechanism of TCR$\gamma\delta$ T cell-mediated suppression of TCR$\alpha\beta$ IEL in the murine colitis model (16). Taken together, these results indicate that it is of great worth to investigate when and how AM regulates the function of TCR$\gamma\delta$ IEL during the development of colitis.

A possible alternative mechanism of AM-mediated suppression of colitis is modification of intestinal microbial flora through its antibacterial activity. Although the etiology of IBD is unknown, an abnormal inflammatory response directed against enteric microbial flora in susceptible hosts has been reported (9). AM has potent antibacterial activity against a variety of Gram-positive and Gram-negative bacteria that are frequently detected in the skin, digestive tract and airways (7, 24), and it has been suggested that the antibacterial activity is enhanced by post-secretory processing of the AM protein (24). Our results show that, after induction of DSS colitis, the number of intestinal anaerobes decreases in the AM-treated compared to the control mice, suggesting that AM suppresses colitis induction through modification of intestinal microbial flora by its antibacterial activity. Since AM is present in epithelium and mucosa in the gastrointestinal tract, it could also prevent the development of colitis in healthy individuals through its antibacterial activity.

Colitis may influence EC immune functions such as the production of cytokines, chemokines, and defensins

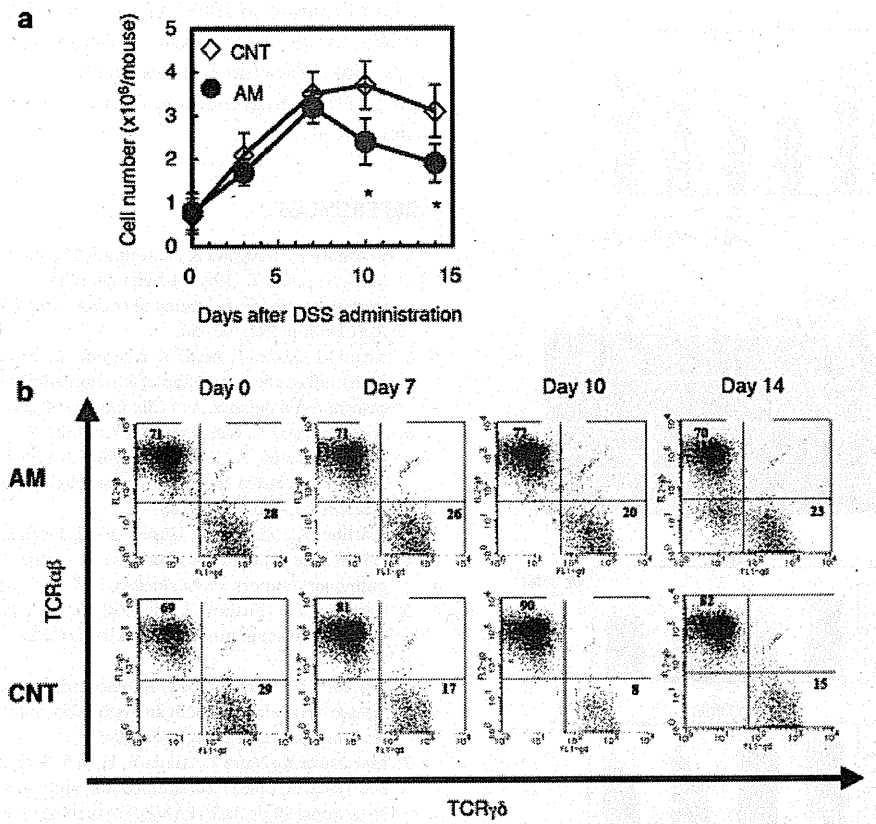

Fig. 4. Alteration of the number and proportion of IEL in the large intestine of mice with DSS-induced colitis treated with AM. (a) Number of CD3-positive IEL. IEL were collected on days 3, 7, 10 and 14 with or without AM administration. IEL were stained with antibodies against CD3, TCRβ and TCR$\gamma\delta$, followed by FACS analysis. Absolute CD3-positive cell number was calculated by multiplying total IEL number by proportion of CD3+-cells. *Represents a statistically significant difference ($P < 0.05$). (b) The proportion of IEL bearing TCR $\alpha\beta$ and TCR $\gamma\delta$. These TCR $\alpha\beta$ and TCR $\gamma\delta$ expressions on IEL are shown after the analysis gate was set on CD3$^+$ cells. Three mice were used for each point. Representative data are shown.

(46, 47), resulting in damage to the physical barrier function of EC. To maintain homeostasis and preserve the integrity of the epithelial barrier, the intercellular junctional complex, consisting of tight junctions, adherens junctions, desmosomes and gap junctions, is thought to facilitate appropriate communication between the external and internal environments. Using the human intestinal cell line, HT-29/B6, inflammatory cytokines such as IFN-γ and TNF-α have been reported to down-regulate the occludin promoter (48). Indeed, abnormal mucosal permeability attributed to inflammation and altered epithelial paracellular permeability has been observed in IBD patients with diarrhea (49, 50). Increased paracellular permeability enhances antigenic exposure to underlying immune cells, further compromising barrier function. In the present study, it was shown that mRNA concentrations of E-cadherin and occludin, which were decreased in the DSS-treated mice, recovered through AM administration, indicating that AM is linked to maintenance of the epithelial barrier against a Th1-type response.

The present results indicate that AM is a potential new therapeutic agent for colitis, and works through anti-inflammatory activity and maintenance of the colonic epithelial barrier concomitantly with its antibacterial effect.

ACKNOWLEDGMENTS

This study was supported by Grants-in-Aid for Scientific Research (C) from the Ministry of Education, Culture, Sports, Science and Technology of Japan (20599015), and the Takeda Science Foundation (K. I-O), in part by grants-in-aid for Scientific Research and for the 21st Century Centers of Excellence Program (Life Science) from the Ministry of Education, Culture, Sports Science and Technology of Japan, the Industrial Technology Research

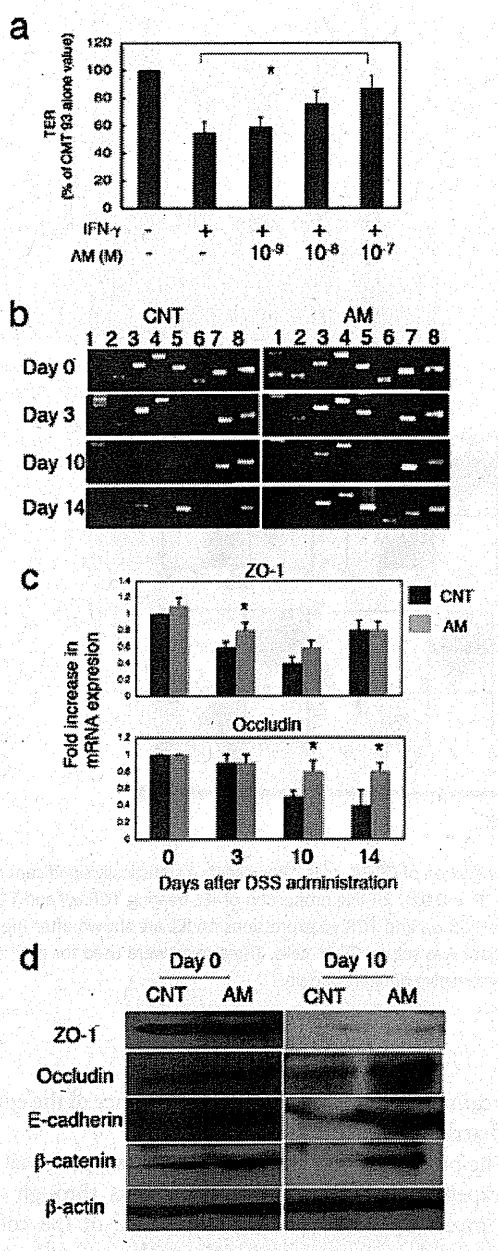

Fig. 5. The colonic epithelial barrier is maintained due to AM administration. (a) Recovery of TER of CMT93 cells by addition of AM. CMT93 cells were exposed to 100 ng/ml of rIFN-γ and a variety of concentration of AM for 24 hr. (b) Recovery of expression of junctional molecules on EC by AM administration to mice with DDS-induced colitis. The amount of mRNA of junction molecules in EC was analyzed by RT-PCR. Lane 1, ZO-1; lane 2, occludin; lane 3, JAM; lane 4, β-catenin; lane 5, E-cadherin; lane 6, desmoglein-2; lane 7, connexin 26; lane 8, β-actin. (c) mRNA expression of ZO-1 and occludin was analyzed quantitatively by real-time PCR. Data is presented as the ratio of degree of expression at each time-point to the data on day 0 in the control mice. *Represents a statistically significant difference between control and AM-treated mice ($P < 0.05$). (d) Western blot analysis of junctional molecules of colonic EC on days 0 and 10 after DSS administration.

Grant Program in 2003 from the New Energy and Industrial Technology Development Organization of Japan, and a research grant for translational research for the Program for Strategic Regional Science and Technology Advancement (K. K.).

REFERENCES

1. Kitamura K., Kangawa K., Kawamoto M., Ichiki Y., Nakamura S., Matsuo H., Eto T. (1993) Adrenomedullin: a novel hypotensive peptide isolated from human pheochromocytoma. *Biochem Biophys Res Commun* **192:** 553–60.
2. Kitani M., Sakata J., Asada Y., Kitamura K., Eto T. (1998) Distribution and expression of adrenomedullin in human gastrointestinal tissue. *Ann Clin Biochem* **35**(Pt 5): 643–8.
3. Asada Y., Hara S., Marutsuka K., Kitamura K., Tsuji T., Sakata J., Sato Y., Kisanuki A., Eto T., Sumiyoshi A. (1999) Novel distribution of adrenomedullin-immunoreactive cells in human tissues. *Histochem Cell Biol* **112:** 185–91.
4. Martinez A., Miller M.J., Unsworth E.J., Siegfried J.M., Cuttitta F. (1995) Expression of adrenomedullin in normal human lung and in pulmonary tumors. *Endocrinology* **136:** 4099–105.
5. Cameron V.A., Fleming A.M. (1998) Novel sites of adrenomedullin gene expression in mouse and rat tissues. *Endocrinology* **139:** 2253–64.
6. Elsasser T.H., Kahl S. (2002) Adrenomedullin has multiple roles in disease stress: development and remission of the inflammatory response. *Microsc Res Tech* **57:** 120–9.
7. Marutsuka K., Nawa Y., Asada Y., Hara S., Kitamura K., Eto T., Sumiyoshi A. (2001) Adrenomedullin and proadrenomedullin N-terminal 20 peptide (PAMP) are present in human colonic epithelia and exert an antimicrobial effect. *Exp Physiol* **86:** 543–5.
8. Ueda S., Nishio K., Minamino N., Kubo A., Akai Y., Kangawa K., Matsuo H., Fujimura Y., Yoshioka A., Masui K., Doi N., Murao Y., Miyamoto S. (1999) Increased plasma levels of adrenomedullin in patients with systemic inflammatory response syndrome. *Am J Respir Crit Care Med* **160:** 132–6.
9. Fiocchi C. (1998) Inflammatory bowel disease: etiology and pathogenesis. *Gastroenterology* **115:** 182–205.
10. Blumberg R.S., Saubermann L.J., Strober W. (1999) Animal models of mucosal inflammation and their relation to human inflammatory bowel disease. *Curr Opin Immunol* **11:** 648–56.
11. Gassler N., Rohr C., Schneider A., Kartenbeck J., Bach A., Obermuller N., Otto H.F., Autschbach F. (2001) Inflammatory bowel disease is associated with changes of enterocytic junctions. *Am J Physiol Gastrointest Liver Physiol* **281:** G216–28.
12. Bouma G., Strober W. (2003) The immunological and genetic basis of inflammatory bowel disease. *Nat Rev Immunol* **3:** 521–33.
13. Cummings J.H., Macfarlane G.T., Macfarlane S. (2003) Intestinal bacteria and ulcerative colitis. *Curr Issues Intest Microbiol* **4:** 9–20.
14. Inagaki-Ohara K., Sasaki A., Matsuzaki G., Ikeda T., Hotokezaka M., Chijiiwa K., Kubo M., Yoshida H., Nawa Y., Yoshimura A. (2006) Suppressor of cytokine signalling 1 in lymphocytes regulates the development of intestinal inflammation in mice. *Gut* **55:** 212–9.
15. Yamamoto M., Fujihashi K., Kawabata K., McGhee J.R., Kiyono H. (1998) A mucosal intranet: intestinal epithelial cells down-regulate intraepithelial, but not peripheral, T lymphocytes. *J Immunol* **160:** 2188–96.
16. Inagaki-Ohara K., Chinen T., Matsuzaki G., Sasaki A., Sakamoto Y., Hiromatsu K., Nakamura-Uchiyama F., Nawa Y., Yoshimura A. (2004) Mucosal T cells bearing TCRgammadelta play a protective role in intestinal inflammation. *J Immunol* **173:** 1390–8.

17. Cheroutre H. (2005) IELs: enforcing law and order in the court of the intestinal epithelium. *Immunol Rev* **206:** 114–31.
18. Komori H.K., Meehan T.F., Havran W.L. (2006) Epithelial and mucosal gamma delta T cells. *Curr Opin Immunol* **18:** 534–8.
19. Inagaki-Ohara K., Dewi F.N., Hisaeda H., Smith A.L., Jimi F., Miyahira M., Abdel-Aleem A.S., Horii Y., Nawa Y. (2006) Intestinal intraepithelial lymphocytes sustain the epithelial barrier function against *Eimeria vermiformis* infection. *Infect Immun* **74:** 5292–301.
20. Ashizuka S., Ishikawa N., Kato J., Yamaga J., Inatsu H., Eto T., Kitamura K. (2005) Effect of adrenomedullin administration on acetic acid-induced colitis in rats. *Peptides* **26:** 2610–5.
21. Gonzalez-Rey E., Fernandez-Martin A., Chorny A., Delgado M. (2006) Therapeutic effect of urocortin and adrenomedullin in a murine model of Crohn's disease. *Gut* **55:** 824–32.
22. Sugimoto K., Ogawa A., Mizoguchi E., Shimomura Y., Andoh A., Bhan A.K., Blumberg R.S., Xavier R.J., Mizoguchi A. (2008) IL-22 ameliorates intestinal inflammation in a mouse model of ulcerative colitis. *J Clin Invest* **118:** 534–44.
23. Inagaki-Ohara K., Sawaguchi A., Suganuma T., Matsuzaki G., Nawa Y. (2005) Intraepithelial lymphocytes express junctional molecules in murine small intestine. *Biochem Biophys Res Commun* **331:** 977–83.
24. Allaker R.P., Grosvenor P.W., McAnerney D.C., Sheehan B.E., Srikanta B.H., Pell K., Kapas S. (2006) Mechanisms of adrenomedullin antimicrobial action. *Peptides* **27:** 661–6.
25. Fuss I.J., Neurath M., Boirivant M., Klein J.S., de la Motte C., Strong S.A., Fiocchi C., Strober W. (1996) Disparate CD4+ lamina propria (LP) lymphokine secretion profiles in inflammatory bowel disease. Crohn's disease LP cells manifest increased secretion of IFN-gamma, whereas ulcerative colitis LP cells manifest increased secretion of IL-5. *J Immunol* **157:** 1261–70.
26. Podolsky D.K. (1991) Inflammatory bowel disease (1). *N Engl J Med* **325:** 928–37.
27. Rogler G., Andus T. (1998) Cytokines in inflammatory bowel disease. *World J Surg* **22:** 382–9.
28. Leonard W.J., O'Shea J.J. (1998) Jaks and STATs: biological implications. *Annu Rev Immunol* **16:** 293–322.
29. Atreya R., Neurath M.F. (2008) Signaling molecules: the pathogenic role of the IL-6/STAT-3 trans signaling pathway in intestinal inflammation and in colonic cancer. *Curr Drug Targets* **9:** 369–74.
30. Schreiber S., Rosenstiel P., Hampe J., Nikolaus S., Groessner B., Schottelius A., Kuhbacher T., Hamling J., Folsch U.R., Seegert D. (2002) Activation of signal transducer and activator of transcription (STAT) 1 in human chronic inflammatory bowel disease. *Gut* **51:** 379–85.
31. Inagaki-Ohara K., Hanada T., Yoshimura A. (2003) Negative regulation of cytokine signaling and inflammatory diseases. *Curr Opin Pharmacol* **3:** 435–42.
32. Mombaerts P., Mizoguchi E., Grusby M.J., Glimcher L.H., Bhan A.K., Tonegawa S. (1993) Spontaneous development of inflammatory bowel disease in T cell receptor mutant mice. *Cell* **75:** 274–82.
33. Chen Y., Chou K., Fuchs E., Havran W.L., Boismenu R. (2002) Protection of the intestinal mucosa by intraepithelial gamma delta T cells. *Proc Natl Acad Sci U S A* **99:** 14338–43.
34. Berkes J., Viswanathan V.K., Savkovic S.D., Hecht G. (2003) Intestinal epithelial responses to enteric pathogens: effects on the tight junction barrier, ion transport, and inflammation. *Gut* **52:** 439–51.
35. Schneeberger E.E., Lynch R.D. (2004) The tight junction: a multifunctional complex. *Am J Physiol Cell Physiol* **286:** C1213–28.
36. Axelsson L.G., Landstrom E., Goldschmidt T.J., Gronberg A., Bylund-Fellenius A.C. (1996) Dextran sulfate sodium (DSS) induced experimental colitis in immunodeficient mice: effects in CD4(+) -cell depleted, athymic and NK-cell depleted SCID mice. *Inflamm Res* **45:** 181–91.
37. Dieleman L.A., Ridwan B.U., Tennyson G.S., Beagley K.W., Bucy R.P., Elson C.O. (1994) Dextran sulfate sodium-induced colitis occurs in severe combined immunodeficient mice. *Gastroenterology* **107:** 1643–52.
38. Egger B., Bajaj-Elliott M., MacDonald T.T., Inglin R., Eysselein V.E., Buchler M.W. (2000) Characterisation of acute murine dextran sodium sulphate colitis: cytokine profile and dose dependency. *Digestion* **62:** 240–8.
39. Powrie F., Carlino J., Leach M.W., Mauze S., Coffman R.L. (1996) A critical role for transforming growth factor-beta but not interleukin 4 in the suppression of T helper type 1-mediated colitis by CD45RB(low) CD4+ T cells. *J Exp Med* **183:** 2669–74.
40. Neurath M.F., Fuss I., Kelsall B.L., Presky D.H., Waegell W., Strober W. (1996) Experimental granulomatous colitis in mice is abrogated by induction of TGF-beta-mediated oral tolerance. *J Exp Med* **183:** 2605–16.
41. Kitani A., Fuss I.J., Nakamura K., Schwartz O.M., Usui T., Strober W. (2000) Treatment of experimental (Trinitrobenzene sulfonic acid) colitis by intranasal administration of transforming growth factor (TGF)-beta1 plasmid: TGF-beta1-mediated suppression of T helper cell type 1 response occurs by interleukin (IL)-10 induction and IL-12 receptor beta2 chain downregulation. *J Exp Med* **192:** 41–52.
42. Ehrhardt R.O., Strober W., Harriman G.R. (1992) Effect of transforming growth factor (TGF)-beta 1 on IgA isotype expression. TGF-beta 1 induces a small increase in sIgA+ B cells regardless of the method of B cell activation. *J Immunol* **148:** 3830–6.
43. Fujihashi K., Kawabata S., Hiroi T., Yamamoto M., McGhee J.R., Nishikawa S., Kiyono H. (1996) Interleukin 2 (IL-2) and interleukin 7 (IL-7) reciprocally induce IL-7 and IL-2 receptors on gamma delta T-cell receptor-positive intraepithelial lymphocytes. *Proc Natl Acad Sci U S A* **93:** 3613–8.
44. Inagaki-Ohara K., Nishimura H., Mitani A., Yoshikai Y. (1997) Interleukin-15 preferentially promotes the growth of intestinal intraepithelial lymphocytes bearing gamma delta T cell receptor in mice. *Eur J Immunol* **27:** 2885–91.
45. Komano H., Fujiura Y., Kawaguchi M., Matsumoto S., Hashimoto Y., Obana S., Mombaerts P., Tonegawa S., Yamamoto H., Itohara S., *et al.* (1995) Homeostatic regulation of intestinal epithelia by intraepithelial gamma delta T cells. *Proc Natl Acad Sci USA* **92:** 6147–51.
46. Campbell N., Yio X.Y., So L.P., Li Y., Mayer L. (1999) The intestinal epithelial cell: processing and presentation of antigen to the mucosal immune system. *Immunol Rev* **172:** 315–24.
47. O'Neil D.A., Porter E.M., Elewaut D., Anderson G.M., Eckmann L., Ganz T., Kagnoff M.F. (1999) Expression and regulation of the human beta-defensins hBD-1 and hBD-2 in intestinal epithelium. *J Immunol* **163:** 6718–24.
48. Mankertz J., Tavalali S., Schmitz H., Mankertz A., Riecken E.O., Fromm M., Schulzke J.D. (2000) Expression from the human occludin promoter is affected by tumor necrosis factor alpha and interferon gamma. *J Cell Sci* **113**(Pt 11): 2085–90.
49. Teahon K., Smethurst P., Levi A.J., Menzies I.S., Bjarnason I. (1992) Intestinal permeability in patients with Crohn's disease and their first degree relatives. *Gut* **33:** 320–3.
50. Irvine E.J., Marshall J.K. (2000) Increased intestinal permeability precedes the onset of Crohn's disease in a subject with familial risk. *Gastroenterology* **119:** 1740–4.

NEPHROLOGY 2009; 14, 80–85 doi:10.1111/j.1440-1797.2008.01006.x

Original Article

Effects of uroguanylin on natriuresis in experimental nephrotic rats

AKIKO BABA, SHOUICHI FUJIMOTO, MASAO KIKUCHI, TOSHIHIRO KITA and KAZUO KITAMURA

Department of Internal Medicine, Division of Circulatory and Body Fluid Regulation, Faculty of Medicine, University of Miyazaki, Japan

SUMMARY:

Aim: Uroguanylin, isolated from human and opossum urine, is a candidate intestinal natriuretic hormone that controls the sodium and water balance between the intestine and the kidneys. Levels of immunoreactive (ir)-uroguanylin in the plasma and urine are increased in rats and humans with nephrotic syndrome, which is physiologically characterized by sodium retention with massive proteinuria. The present study evaluates the effect of natriuresis induced by uroguanylin on nephrotic rats.

Methods: Normal rats and rats rendered nephrotic by injections of puromycin aminonucleoside (PAN) were treated with uroguanylin (0.5 nmol/h, delivered by an osmotic pump) or with vehicle during the sodium retention phase. All rats consumed the same quantity of sodium.

Results: Uroguanylin did not increase urinary excretion of sodium and water in normal rats, but significantly increased urinary sodium excretion during the sodium retention phase in nephrotic rats (untreated vs uroguanylin-treated nephrotic rats in mmol/mmol creatinine; 2.92 ± 0.65 vs 8.93 ± 2.53 on day 6, $P < 0.05$; 3.55 ± 0.47 vs 10.37 ± 1.73 on day 7, $P < 0.01$; 14.88 ± 2.32 vs 24.47 ± 2.86 on day 8, $P < 0.05$). Plasma levels of ir-uroguanylin in uroguanylin-treated nephrotic rats on day 6 were significantly increased compared with those in uroguanylin-treated control and untreated nephrotic rats.

Conclusion: Uroguanylin increased urinary sodium excretion in rats with PAN-induced nephrosis, and might be useful for treating sodium retention in patients with nephrotic syndrome.

KEY WORDS: **natriuresis, nephrotic syndrome, PAN-induced nephrosis, sodium retention, uroguanylin.**

The endogenous peptide uroguanylin, belonging to the growing family of natriuretic peptides that activate transmembranous guanylate cyclase (GC)-C, influences cellular function via the intracellular second messenger, cyclic guanosine 3′-5′ monophosphate (cGMP) and affects water and electrolyte transport.[1–3] This mechanism of uroguanylin in the intestine is established, but the situation is quite different in the kidney. Indeed, uroguanylin stimulates the urinary excretion of sodium, potassium and water in the isolated perfused rat kidney[4] and in mice *in vivo*,[5,6] but the effects of uroguanylin are unaltered in GC-C-deficient mice.[7] This finding suggests that uroguanylin functions through GC-C independent signalling pathways in the kidney.

Although the detailed mechanism is unknown, accumulating data indicates that uroguanylin could be an important natriuretic factor in various states including nephrosis. We previously found that uroguanylin excretion in urine is increased in humans and rats on a high-salt diet compared with a low-salt one, and that uroguanylin mRNA expression is increased in the intestine and kidneys of rats given a high-salt diet.[8,9] In addition, natriuresis induced by oral salt loading is decreased in uroguanylin-deficient mice.[10] Uroguanylin levels are also increased in the circulation of patients with renal disease and congestive heart failure.[11–14] We recently examined relationships between urinary immunoreactive (ir)-uroguanylin and sodium excretion in rats with puromycin aminonucleoside (PAN)-induced nephrosis.[15] That study showed that urinary excretion of ir-uroguanylin increased by approximately eightfold or more in rats with PAN-induced nephrosis compared with controls during the natriuretic phase, in accordance with an increase

Correspondence: Dr Akiko Baba, Division of Circulatory and Body Fluid Regulation, Department of Internal Medicine, Faculty of Medicine, University of Miyazaki, Kihara 5200, Kiyotake, Miyazaki 889-1692, Japan. Email: akikob@fc.miyazaki-u.ac.jp

Accepted for publication 27 May 2008.

of plasma ir-uroguanylin. However, uroguanylin mRNA in the intestine never increased, indicating that uroguanylin acts in the kidney as an autocrine and/or paracrine factor.

Uroguanylin probably participates in regulation of the sodium balance in the kidney. However, the natriuretic effects of uroguanylin as a therapeutic agent under sodium and water retention have not been investigated. This study evaluates whether exogenous uroguanylin administration induces natriuresis during the period of sodium retention in rats with PAN-induced nephrosis.

METHODS

Animals and peptide

Male Sprague–Dawley rats (Charles River, Kanagawa, Japan) weighing 160–230 g were housed in a temperature and light-controlled environment with a 12:12 h light : dark cycle and placed in individual metabolic cages 1 day before starting experiments. Nephrotic rats were allowed free access to standard rat chow (Nihon CLEA, Tokyo, Japan) and water throughout the study, whereas pair-fed control animals had free access to water but received the mean daily intake of the corresponding nephrotic rats. Rat uroguanylin was provided by the Peptide Institute (Osaka, Japan).

Experimental protocol

In study 1, the rats were randomized into four groups as follows: untreated controls (group I, $n = 6$); uroguanylin-treated controls (group II, $n = 6$); untreated nephrotic rats (group III, $n = 10$); and uroguanylin-treated nephrotic rats (group IV, $n = 10$). Nephrosis was induced by a single i.p. injection of 150 mg/kg of PAN (Sigma, St Louis, MO, USA) dissolved in saline (day 0). Control groups were injected with an equivalent volume of saline.

On day 4, the treated rats were anaesthetized with pentobarbital sodium, and i.p. implanted with micro-osmotic pumps (model 1003D; Durect, Cupertino, CA, USA) that were scheduled to release 0.5 nmol/h of rat uroguanylin in water over 3 days. The untreated groups were similarly infused with vehicle. The timing of uroguanylin administration was matched to the sodium retention phase[15] when uroguanylin excretion peaks and is followed by natriuresis in nephrotic rats. The dose of uroguanylin was adjusted to produce an equivalent peak in normal rats to that expected in nephrotic rats.

Urinary sodium, protein, creatinine, ir-uroguanylin and cyclic guanylic acid (cGMP) were measured in 24 h urine samples. Urinary sodium, protein and creatinine were measured by indirect potentiometry using an automatic analyzer with ion-selective electrodes, by colourimetric reactions using pyrogallol red and by the enzymatic assay, respectively.

In study 2, 48 rats ($n = 6$/group × four groups × two sets) were treated in the same way as in study 1 and then killed for blood and tissue sampling on days 6 and 12. Blood was collected into chilled polypropylene tubes containing ethylenediaminetetraacetic acid (EDTA)-2Na (1 mg/mL blood) and aprotinin (500 units/mL blood), then immediately centrifuged at 1700 *g* for 15 min at 4°C. The kidneys and upper small intestines were resected and frozen for RNA extraction and cGMP assays. Differences in the circadian expression of uroguanylin were avoided by standardizing the experimental schedule for both groups.

All experiments described above proceeded according to the regulations established by the Animal Research Committee of Miyazaki University.

Uroguanylin and cGMP assays

The uroguanylin radioimmunoassay (RIA) for plasma and urine proceeded as described by Fukae *et al.*[8] This RIA specifically recognizes uroguanylin and prouroguanylin, both of which contain reduced and S-carboxymethylated (RCM) forms.

Tissues and urinary cGMP concentrations were determined using a cGMP enzyme-linked immunosorbent assay (ELISA). Samples were homogenized or precipitated with 6% trichloroacetic acid (TCA) on ice. The supernatant was washed with water-saturated diethyl ether to remove the TCA. The residue was evaporated to dryness, reconstituted in assay buffer and measured using an ELISA kit (GE Healthcare, Buckinghamshire, UK).

Real-time reverse transcriptase-polymerase chain reaction

Total RNA (5 μg) extracted using the total RNA Isolation Reagent (Invitrogen, Carlsbad, CA, USA) was reverse-transcribed using Superscript Reverse Transcriptase (Invitrogen) into cDNA. Rat uroguanylin mRNA levels were measured by Real-Time Quantitative PCR (ABI Prism 7700 Sequence Detector; Applied Biosystems, Foster City, CA, USA) as described.[15] The cDNA was amplified using forward and reverse oligonucleotide primers, and probes were quenched with 6-carboxytetramethyl-rhodamine. Levels of uroguanylin mRNA were normalized to those of internal control glyceraldehyde 3-phosphate dehydrogenase (GAPDH) mRNA. All polymerase chain reaction (PCR) products were verified once by sequencing and all reactions proceeded in duplicate.

Statistical analysis

All data are presented as means ± standard error of the mean. We applied the one-way ANOVA to compare parametric data among the four groups. Significances of individual differences were evaluated by using the Tukey–Kramer test if the ANOVA findings were significant. $P < 0.05$ was considered statistically significant in all calculations.

RESULTS

In study 1, PAN-induced nephrosis affected urinary sodium excretion and urinary ir-uroguanylin excretion (Fig. 1). The urinary sodium excretion was decreased during the early phase (sodium retention) and increased later (natriuretic phase) in nephrotic rats. Urinary ir-uroguanylin excretion was increased in nephrotic compared with control rats without uroguanylin administration on days 9–12.

Uroguanylin did not increase urinary sodium excretion in control rats (Fig. 2a). On the other hand, exogenous uroguanylin increased urinary sodium excretion in the nephrotic groups on days 6–8 (Fig. 2b; group III vs group IV in mmol/mmol creatinine; 2.92 ± 0.65 vs 8.93 ± 2.53 on day 6, $P < 0.05$; 3.55 ± 0.47 vs 10.37 ± 1.73 on day 7, $P < 0.01$; and 14.88 ± 2.32 vs 24.47 ± 2.86 on day 8, $P < 0.05$).

The urinary excretion of ir-uroguanylin during uroguanylin administration was obviously increased in groups II and IV, and the peak of ir-uroguanylin in normal rats (group II) was comparable with the natriuretic phase of nephrotic rats (group III) (Fig. 3).

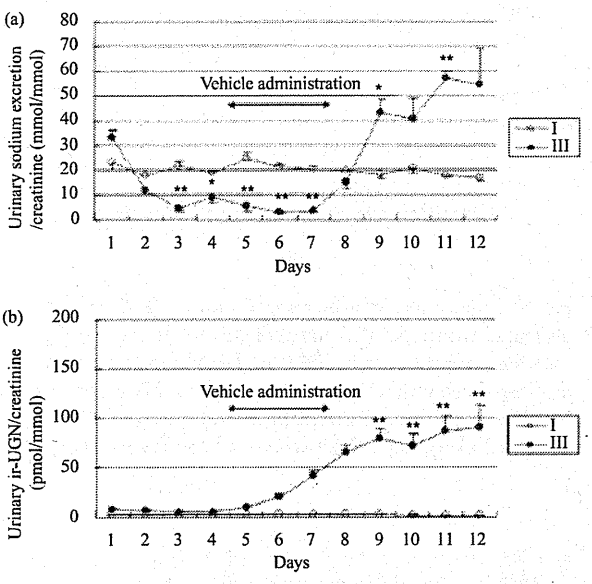

Fig. 1 Time course of urinary sodium excretion (a) and immunoreactive-uroguanylin (ir-UGN) (b) in normal and nephrotic rats without exogenous uroguanylin. Group I, untreated control rats. (○) $n = 6$. Group III, untreated nephrotic rats. (●) $n = 10$. Values are means ± standard error of the mean. $^{*}P < 0.05$; $^{**}P < 0.01$; compared with group I. One-way ANOVA and Tukey–Kramer test.

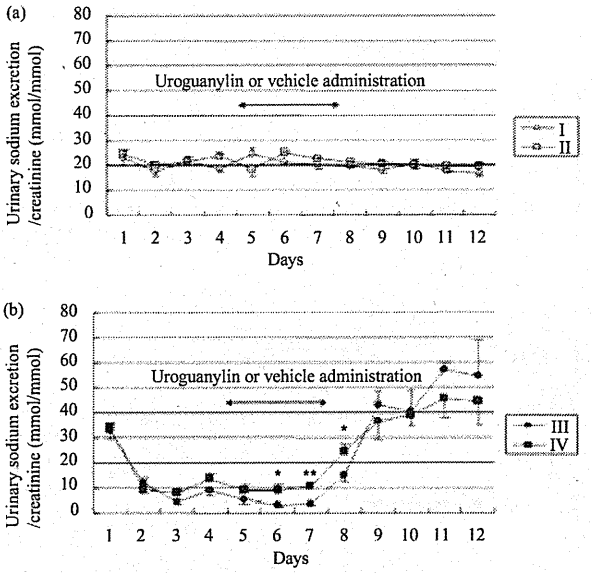

Fig. 2 Time course of urinary sodium excretion in control (a) and nephrotic (b) groups. Groups I, II, III and IV: (○) untreated controls; (□) uroguanylin-treated controls; (●) untreated nephrotic rats; and (■) uroguanylin-treated nephrotic rats respectively ($n = 6$, groups I and II; $n = 10$, groups III and IV). Values are means ± standard error of the mean (SEM). $^{*}P < 0.05$; $^{**}P < 0.01$; compared with group I (a) or group III (b). One-way ANOVA and Tukey–Kramer test.

Urine volume was significantly increased in the nephrotic rats (group III) compared with the control (phase of natriuresis) rats on days 8–11 (Fig. 4). However, exogenously administrated uroguanylin did not potentiate diuresis in the nephrotic groups (group III vs IV; Fig. 4). Both nephrotic groups developed proteinuria (Fig. 5), but exogenous uroguanylin did not alter the level of proteinuria in the nephrotic rats (group III vs IV, 453 ± 36.4 vs 444 ± 48.3 mg/day, on day 7). Urinary excretion of cGMP, the second messenger of uroguanylin, was decreased in the nephrotic rats compared with normal rats (Fig. 6), but this was not increased in uroguanylin-treated or untreated groups.

In study 2, Figure 7 compares the plasma concentration of ir-uroguanylin among the four groups. Uroguanylin administration increased the plasma level of ir-uroguanylin in control rats on day 6 (group I vs II), but the difference did not reach significance. The plasma level of ir-uroguanylin in nephrotic rats was increased in group IV compared with group III (group III vs group IV, 3.4 ± 0.6 vs 7.0 ± 0.7 pmol/mL, $P < 0.01$). The plasma ir-uroguanylin concentrations were similar in groups II and III. At day 12, plasma ir-uroguanylin levels did not differ among the four groups.

Nephrosis induction and/or uroguanylin administration did not increase tissue cGMP concentrations (groups I, II, III and IV: 15.31 ± 1.18, 20.67 ± 5.54, 25.33 ± 1.95 and 17.70 ± 3.94 fmol/mg tissue weight, respectively).

Uroguanylin mRNA expression in the kidneys on day 6 was decreased in nephrotic groups on day 6 (group I vs III: 100 ± 13.3 vs 49.5 ± 10.0%, $P < 0.05$ respectively) (Fig. 8a), and was unaffected by uroguanylin administration in nephrotic rats. On the other hand, expression levels in the intestines did not differ among the four groups (groups I, II, III and IV: 100 ± 19.3%, 120.0 ± 3.9%, 106.4 ± 18.8% and 97.7 ± 8.8%) (Fig. 8b).

DISCUSSION

Uroguanylin induces natriuresis in the isolated perfused kidney[4] and *in vivo*.[5,6] We previously found that urinary sodium excretion abruptly increases immediately after the period of retention in nephrotic syndrome, in accordance with increased urinary uroguanylin excretion.[15] However, whether exogenous uroguanylin elicits an increase in urinary sodium under pathological conditions with sodium retention remains unclear. The present study discovered that continuous, i.p. administration of uroguanylin induced increased sodium excretion into the urine during the period of sodium retention in nephrotic rats. Sodium and water retention comprise a major clinical problem in the management of patients with nephrotic syndrome, in which natriuresis by loop diuresis or atrial natriuretic peptide (ANP) is obviously attenuated.[16–18] Although further studies are

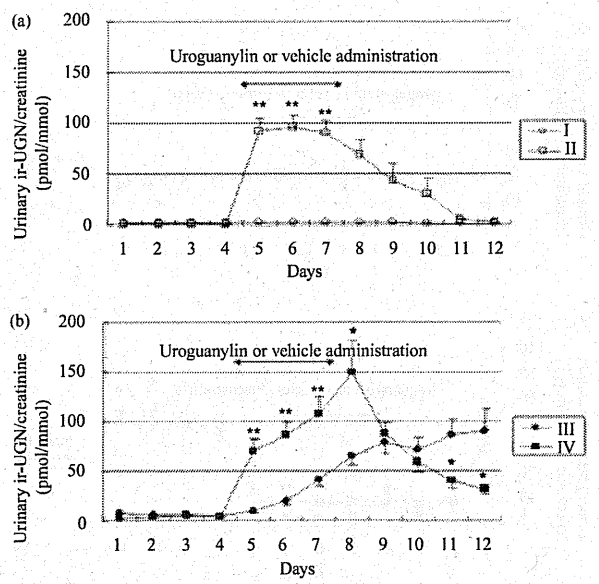

Fig. 3 Time course of urinary immunoreactive-uroguanylin (ir-UGN) excretion in control (a) and in nephrotic (b) rats. Groups I, II, III and IV: (○) untreated controls; (□) uroguanylin-treated controls; (●) untreated nephrotic rats; (■) uroguanylin-treated nephrotic rats respectively ($n = 6$, groups I and II; $n = 10$, groups III and IV). Values are means ± standard error of the mean. $^{*}P < 0.05$; $^{**}P < 0.01$; compared with group I (a) or group III (b). One-way ANOVA and Tukey–Kramer test.

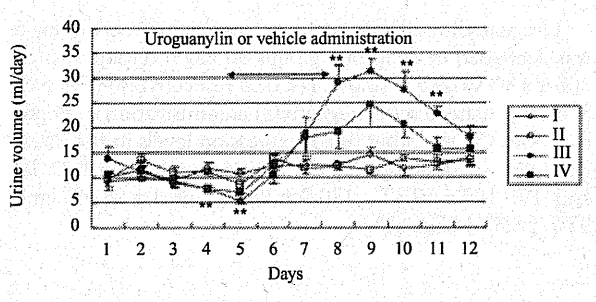

Fig. 4 Time course of urine volume. Groups I, II, III and IV: (○) untreated controls; (□) uroguanylin-treated controls; (●) untreated nephrotic rats; (■) uroguanylin-treated nephrotic rats respectively ($n = 6$, groups I and II; $n = 10$, groups III and IV). Values are means ± standard error of the mean. $^{**}P < 0.01$, compared with group I. One-way ANOVA and Tukey–Kramer test.

needed to verify the notion, uroguanylin might improve natriuretic activity in patients with nephrotic syndrome.

Uroguanylin did not promote sodium excretion in normal rats at the same dose as that administrated to nephrotic rats. The dose of uroguanylin administration in this study was lower than that of previous studies,[4–6] and might be insufficient to induce natriuresis. The plasma ir-uroguanylin concentration on day 6 was significantly

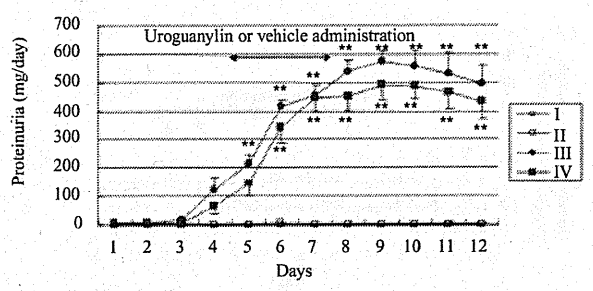

Fig. 5 Time course of proteinuria. Groups I, II, III and IV: (○) untreated controls; (□) uroguanylin-treated controls; (●) untreated nephrotic rats; (■) uroguanylin-treated nephrotic rats respectively ($n = 6$, groups I and II; $n = 10$, groups III and IV). Values are means ± standard error of the mean. $^{**}P < 0.01$, compared with group I. One-way ANOVA and Tukey–Kramer test.

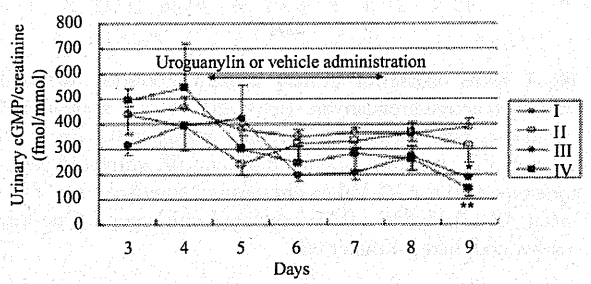

Fig. 6 Urinary cyclic 3′,5′-guanosine monophosphate (cGMP) excretion. Groups I, II, III and IV: (○) untreated controls; (□) uroguanylin-treated controls; (●) untreated nephrotic rats; (■) uroguanylin-treated nephrotic rats respectively ($n = 4$). Values are means ± standard error of the mean. $^{*}P < 0.05$; $^{**}P < 0.01$; compared with group I. One-way ANOVA and Tukey–Kramer test.

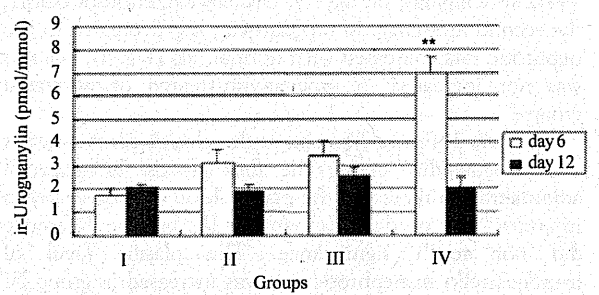

Fig. 7 Plasma concentration of immunoreactive (ir)-uroguanylin on days 6 (□) and 12 (■). Groups I, II III and IV: untreated controls, uroguanylin-treated controls, untreated nephrotic and uroguanylin-treated nephrotic rats respectively ($n = 6$). Values are means ± standard error of the mean. $^{**}P < 0.01$ compared with other groups. One-way ANOVA and Tukey–Kramer test.

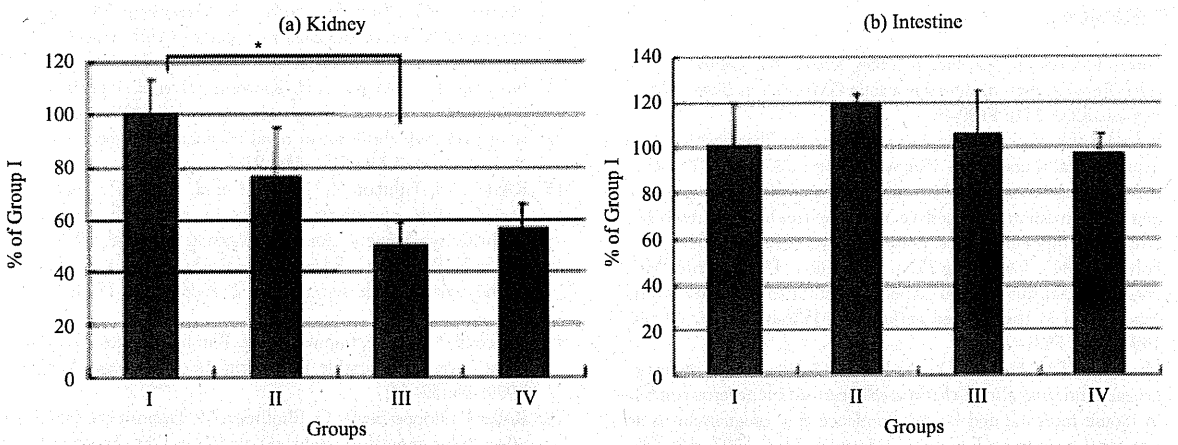

Fig. 8 Comparison in renal (a) and intestinal (b) uroguanylin mRNA expression on day 6. Groups I, II, III and IV: untreated controls, uroguanylin-treated controls, untreated nephrotic and uroguanylin-treated nephrotic rats, respectively ($n = 6$). Values are means ± standard error of the mean. *$P < 0.05$ compared with group I. One-way ANOVA and Tukey–Kramer test.

increased only in uroguanylin-treated nephrotic rats (Fig. 7), in which natriuresis was significant (Fig. 2). Additionally, sodium excretion was significantly suppressed during the sodium retention phase (Fig. 1) in nephrotic rats, and uroguanylin administration partially reversed this suppression, but the value did not increase to the normal range in nephrotic rats (Fig. 2). The status of the sodium balance could influence the sensitivity of the kidney to uroguanylin. However, further studies are required to clarify this notion.

Increased production and/or a decrease in uroguanylin metabolism would be required to increase the plasma ir-uroguanylin concentration in nephrosis. However, the level of uroguanylin mRNA in the intestine was not changed among the four groups and that in the kidney had not increased in nephrotic rats on day 6 (Fig. 8). These results suggested that uroguanylin production does not always increase in nephrosis. The excretion of exogenously administrated uroguanylin into the urine persisted for 3 days after termination (Fig. 3), so uroguanylin might be retained for longer in plasma, thus generating a time-lag between uroguanylin production and accumulation. Furthermore, metabolism might be different in nephrosis. We previously showed by reverse-phase high-performance liquid chromatography coupled with RIA that urinary ir-uroguanylin has two major immunoreactive peaks in nephrotic rats.[15] The main form was bioactive uroguanylin and the remainder was a precursor, whereas normal urine has only the bioactive peak. In addition, the plasma and urinary uroguanylin precursor concentration is increased in patients with chronic glomerulonephritis and retained renal function.[11] Thus, the possibility that precursor secretion from the intestine or other organs is increased in nephrotic syndrome could not be excluded.

To clarify whether the receptor is upregulated in nephrotic syndrome, we examined GC-C mRNA expression in the kidneys. However, the levels of GC-C mRNA in the kidney were too low on day 6 to compare uroguanylin-treated and untreated nephrotic rats (data not shown). In addition, urinary excretion and tissues levels of cGMP, an intracellular second messenger of uroguanylin, were not increased in uroguanylin-treated rats (group IV) compared with untreated (group III) nephrotic rats. Uroguanylin signalling in the kidney remains obscure, but our results suggested that uroguanylin acts via a GC-C independent pathway for urinary sodium excretion in nephrosis. Recent reports have indicated that some GC-C independent pathways exist because the effect of uroguanylin on the kidney persists in mice lacking GC-C.[7,19–24] Uroguanylin acts through a GC-C-independent, cGMP-dependent mechanism in mice lacking the GC-C receptor.[7] However, the levels of cGMP did not change in our study, so other cGMP-independent pathways might be associated with nephrosis. ANP, which is one of the most potent of the natriuretic factors, is produced mainly in the cardiac atria and elicits natriuresis by activating the transmembranous guanylate cyclase, GC-A, which results in increased intracellular cGMP. The effect of infused ANP is reduced in nephrotic syndrome because cGMP-phosphodiesterase (PDE) activity, which catabolizes and removes cGMP, is increased in nephrosis.[25] On the other hand, uroguanylin might work via the cGMP-independent pathway, and be able to induce natriuresis in the nephrotic kidney.

In conclusion, uroguanylin increased urinary sodium excretion in rats with PAN-induced nephrosis. Further studies are warranted to clarify the mechanisms of uroguanylin action in the nephrotic kidney. However, uroguanylin plays an important role as a natriuretic factor in nephrotic syndrome, and might be a useful novel agent for treating conditions associated with sodium retention.

ACKNOWLEDGEMENTS

This study was supported by Grants-in-Aid for Scientific Research from the Ministry of Education, Science, Sports and Culture in Japan.

REFERENCES

1. Forte LR, London RM, Freeman RH, Krause WJ. Guanylin peptides: Renal actions mediated by cyclic GMP. *Am. J. Physiol. Renal Physiol.* 2000; **278**: F180–91.
2. Forte LR. Uroguanylin and guanylin peptides: Pharmacology and experimental therapeutics. *Pharmacol. Ther.* 2004; **104**: 137–62.
3. Fan X, Wang Y, London RM *et al.* Signaling pathways for guanylin and uroguanylin in the digestive, renal, central nervous, reproductive, and lymphoid systems. *Endocrinology* 1997; **138**: 4636–48.
4. Fonteles MC, Greenberg RN, Monteiro HAS, Currie MG, Forte LR. Natriuretic and kaliuretic activities of guanylin and uroguanylin in the isolated perfused rat kidney. *Am. J. Physiol.* 1998; **275**: F191–7.
5. Greenberg RN, Hill M, Crytzer J *et al.* Comparison of effects of uroguanylin, guanylin, *Escherichia coli* heart–stable enterotoxin STa in mouse intestine and kidney: Evidence that uroguanylin is an intestinal natriuretic hormone. *J. Investig. Med.* 1997; **45**: 276–82.
6. Carrithers SL, Hill MJ, Johnson BR *et al.* Renal effects of uroguanylin and guanylin *in vivo*. *Braz. J. Med. Biol. Res.* 1999; **32**: 1337–44.
7. Carrithers SL, Ott CE, Hill MJ *et al.* Guanylin and uroguanylin induce natriuresis in mice lacking guanylyl cyclase-C receptor. *Kidney Int.* 2004; **65**: 40–53.
8. Fukae H, Kinoshita H, Fujimoto S, Kita T, Nakazato M, Eto T. Changes in urinary levels and renal expression of uroguanylin on low or high salt diets in rats. *Nephron* 2002; **92**: 373–8.
9. Kita T, Kitamura K, Sakata J, Eto T. Marked increased of guanylin secretion in response to salt loading in the rat small intestine. *Am. J. Physiol.* 1999; **277**: G960–6.
10. Lorenz JN, Nieman M, Sabo J *et al.* Uroguanylin knockout mice have increased blood pressure and impaired natriuretic response to enteral NaCl load. *J. Clin. Invest.* 2003; **112**: 1244–54.
11. Kinoshita H, Fujimoto S, Kita T *et al.* Urine and plasma levels of uroguanylin and its molecular forms in renal disease. *Kidney Int.* 1997; **52**: 1028–34.
12. Kinoshita H, Fujimoto S, Fukae H *et al.* Plasma and urine levels of uroguanylin, a new natriuretic peptide, in nephrotic syndrome. *Nephron* 1999; **81**: 160–64.
13. Carrithers SL, Eber SL, Forte LR, Greenberg RN. Increased urinary excretion of uroguanylin in patients with congestive heart failure. *Am. J. Physiol. Heart Circ. Physiol.* 2000; **278**: H538–47.
14. Nakazato M, Yamaguchi H, Kinoshita H *et al.* Identification of biologically active and inactive human uroguanylin in plasma and urine and their increases in renal insufficiency. *Biochem. Biophys. Res. Commun.* 1996; **220**: 586–93.
15. Kikuchi M, Fujimoto S, Fukae H *et al.* Rule of uroguanylin, a peptide with natriuretic activity, in rats with experimental nephritic syndrome. *J. Am. Soc. Nephrol.* 2005; **16**: 392–7.
16. Perico N, Remuzzi G. Edema of the nephrotic syndrome: The role of the atrial peptide system. *Am. J. Kidney Dis.* 1993; **22**: 355–66.
17. Perico N, Delaini F, Lupini C *et al.* Blunted excretory response to atrial natriuretic peptide in experimental nephrosis. *Kidney Int.* 1989; **36**: 57–64.
18. Keller E, Hoppe-Seyler G, Shollmeyer P. Disposition and diuretic effect of furosemide in nephrotic syndrome. *Clin. Pharmacol. Ther.* 1982; **32**: 442–9.
19. Sindic A, Basoglu C, Cerci A *et al.* Guanylin, uroguanylin, and heat-stable euterotoxin activate guanylate cyclase C and/or a pertussis toxin-sensitive G protein in human proximal tubule cells. *J. Biol. Chem.* 2002; **277**: 17758–64.
20. Sindic A, Velic A, Basoglu C *et al.* Uroguanylin and guanylin regulate transport of mouse cortical collecting duct independent of guanylate cyclase C. *Kidney Int.* 2005; **68**: 1008–17.
21. Sindic A, Hirsch JR, Velic A, Piechota H, Schlatter E. Guanylin and uroguanylin regulate electrocyte transport in isolated human cortical collecting ducts. *Kidney Int.* 2005; **67**: 1420–27.
22. Elitsur N, Lorenz JN, Hawkins JA *et al.* The proximal convoluted tubule is a target for the uroguanylin-regulated natriuretic response. *J. Pediatr. Gastroenterol. Nutr.* 2006; **43**: S74–81.
23. Sindic A, Schlatter E. Cellular effects of guanylin and uroguanylin. *J. Am. Soc. Nephrol.* 2006; **17**: 607–16.
24. Sindic A, Schlatter E. Mechanisms of action of uroguanylin and guanylin and their role in salt handling. *Nephrol. Dial. Transplant.* 2006; **21**: 3007–12.
25. Valentin JP, Ying WZ, Sechi L *et al.* Phosphodiesterase inhibitors correct resistance to natriuretic peptides in rats with Heymann nephritis. *J. Am. Soc. Nephrol.* 1996; **7**: 582–93.

Biochemical and Biophysical Research Communications 384 (2009) 249–254

Contents lists available at ScienceDirect

Biochemical and Biophysical Research Communications

journal homepage: www.elsevier.com/locate/ybbrc

Flow cytometric analysis of the calcitonin receptor-like receptor domains responsible for cell-surface translocation of receptor activity-modifying proteins

Kenji Kuwasako [a,*], Kazuo Kitamura [b], Sayaka Nagata [b], Johji Kato [a]

[a] Frontier Science Research Center, University of Miyazaki, 5200 Kihara, Kiyotake, Miyazaki 889-1692, Japan
[b] Circulation and Body Fluid Regulation, Faculty of Medicine, University of Miyazaki, 5200 Kihara, Kiyotake, Miyazaki 889-1692, Japan

ARTICLE INFO

Article history:
Received 20 April 2009
Available online 24 April 2009

Keywords:
Receptor activity-modifying proteins
Calcitonin receptor-like receptor
Chimeric receptor
Translocation
Flow cytometry

ABSTRACT

The three receptor activity-modifying proteins (RAMPs1, -2, and -3) associate with a wide variety of G protein-coupled receptors (GPCRs), including calcitonin receptor-like receptor (CRLR). In this study, we used flow cytometry to measure RAMP translocation to the cell surface as a marker of RAMP–receptor interaction. Because VPAC2 does not interact with RAMPs, although, like CRLR, it is a Family B peptide hormone receptor, we constructed a set of chimeric CRLR/VPAC2 receptors to evaluate the trafficking interactions between CRLR domains and each RAMP. We found that CRLR regions extending from transmembrane domain 1 (TM1) through TM5 are necessary and sufficient for the transport of RAMPs to the plasma membrane. In addition, the extracellular N-terminal domain of CRLR, its 3rd intracellular loop and/or TM6 were also important for the cell-surface translocation of RAMP2, but not RAMP1 or RAMP3. Other regions within CRLR were not involved in trafficking interactions with RAMPs. These findings provide new insight into the trafficking interactions between accessory proteins such as RAMPs and their receptor partners.

Introduction

Receptor activity-modifying proteins (RAMPs1, -2 and -3) were the first accessory proteins known to modulate the function of G protein-coupled receptors (GPCRs) [1]. In mammals, all three RAMPs are comprised of ~160 amino acids and exhibit a common structure consisting of a large extracellular N-terminal domain, a single membrane-spanning domain and a short cytoplasmic C-terminal tail. However, the three isoforms share less than 30% sequence identity [1,2], differ with respect to their expression levels in tissues, and are differentially affected by various pathological conditions [2].

RAMPs were first identified as chaperones promoting the forward trafficking of calcitonin receptor-like receptor (CRLR; a Family B GPCR) and calcium sensing receptor (a Family C GPCR) from the endoplasmic reticulum to the cell surface [1–3]. Once at the cell surface, RAMPs govern the expression of the GPCR phenotype [2,4]. For example, CRLR/RAMP1 and CRLR/RAMP2 or -3 function as calcitonin gene-related peptide (CGRP) and adrenomedullin (AM) receptors, respectively [1,2]. Both agonists are potent vasodilators that also have been shown to exert powerful protective effects against multi-organ damage [2,5].

RAMPs can also interact strongly with Family B GPCRs able to translocate to the cell surface without a chaperone [2,4]. For example, expression of the calcitonin (CT) receptor with RAMP1, -2 or -3 produces three subtypes of high-affinity amylin receptor [2,4]. All three RAMPs strongly interact with the vasoactive intestinal peptide (VIP)/pituitary adenylate cyclase-activating polypeptide type 1 receptor (VPAC1) with no effect on the receptor's pharmacology [2,4]. The parathyroid hormone 1 (PTH1) and glucagon receptors are known to selectively interact with RAMP2, while the PTH2 receptor selectively interacts with RAMP3 [2,4].

We previously demonstrated the utility of flow cytometry for evaluating the trafficking interactions between CRLR and various RAMP mutants [6,7]. However, little is known about the trafficking interactions between specific CRLR domains and each of three RAMPs. In the present study, therefore, we generated chimeric receptors by exchanging regions of CRLR with the corresponding sequences of VPAC2, which our flow cytometric analysis showed does not interact with any V5-tagged RAMPs in human embryonic kidney (HEK)-293 cells. Our analysis revealed not only the key CRLR domains responsible for cell-surface translocation of each RAMP, but also differences in the RAMP–CRLR interactions among the three RAMPs.

* Corresponding author. Fax: +81 985 85 9718.
E-mail address: kuwasako@fc.miyazaki-u.ac.jp (K. Kuwasako).

0006-291X/$ - see front matter © 2009 Elsevier Inc. All rights reserved.
doi:10.1016/j.bbrc.2009.04.097

Materials and methods

Regents and antibodies. Human (h)VIP and αCGRP were purchased from the Peptide Institute (Osaka, Japan). Human AM was kindly donated by Shionogi & Co. (Osaka, Japan). Mouse anti-V5 antibody and FITC-conjugated mouse anti-V5 monoclonal antibody (anti-V5-FITC antibody) were purchased from Invitrogen.

Expression constructs and chimers. Human VPAC2 (GenBank Accession No. L40764) was cloned from cDNA obtained from human small intestine (Clonthech) by PCR using appropriate primers and then modified to provide a consensus Kozak sequence as previously described [8]. The expression vector pCAGGS-VPAC2 was then constructed by cloning VPAC2 cDNA into the mammalian vector pCAGGS/Neo using the 5′ XhoI and 3′ NotI sites [8]. In addition, a double V5 epitope tag was ligated, in-frame, to the 5′ end of the VPAC2 cDNA, and the native signal sequences were replaced with the influenza hemagglutinin signal sequence [8], after which the V5-VPAC2 was cloned into pCAGGS/Neo. In similar fashion, wild-type and double V5-tagged constructs for hCRLR and each RAMP were cloned into pCAGGS/Neo [6,9]. Because V5-RAMP3 was more strongly expressed at the cell surface than V5-RAMP1 or -2, even when transfected alone into HEK-293 cells [6], a double V5 epitope tag was inserted between amino acids 33 and 34 in the hRAMP3 N-terminus, as described previously [10].

Nine CRLR/VPAC2 chimeras (CH1–CH9) were constructed utilizing seven restriction sites. Human CRLR naturally possesses three sites (at two positions distal to the N-terminus and TM2, respectively and at a position proximal to the C-terminus); the remaining four sites (at positions distal to TM3, -4, -5 and -6, respectively) were introduced without altering the amino acid sequence of the receptor. VPAC2 shares only 30% amino acid sequence identity with hCRLR and contains none of these sites. Therefore, corresponding VPAC2 fragments containing these restriction sites were prepared by PCR using primers containing the sites. The separate fragments of CRLR and VPAC2 were then ligated into the same expression vector.

The aforementioned gene constructs were all sequenced using an Applied Biosystems 310 Genetic Analyzer.

Cell culture and DNA transfection. HEK-293 or COS-7 cells were maintained in DMEM supplemented with 10% FBS, 100 U/ml penicillin G, 100 μg/ml streptomycin, 0.25 μg/ml amphotericin B at 37 °C under a humidified atmosphere of 95% air/5% CO_2. For experimentation, cells were seeded into 12- or 24-well plates and, upon reaching 70–80% confluence, were transiently transfected with the indicated cDNAs using LipofectAMINE transfection reagents (Invitrogen) according to the manufacturer's instructions. Expression vector constructs for the appropriate wild-type or chimeric receptor and each RAMP were cotransfected in equal amounts. As a control, some cells were transfected with empty vector (pCAGGS/Neo) (*Mock*). All of the experiments were performed 48 h after transfection.

Fluorescence-activated cell-sorting (FACS) analysis. To evaluate cell surface expression of the indicated V5-tagged constructs, cells grown in 12-well plates were harvested following transient transfection, washed twice with PBS, resuspended in ice-cold FACS buffer [8], and then incubated for 60 min at 4 °C in the dark with anti-V5-FITC antibody (1:1000 dilution). For evaluation of intracellular and/or surface expression of the aforementioned V5-tagged constructs, HEK-293 cells were first permeabilized using IntraPrep™ reagents (Beckman Coulter) according to the manufacturer's instructions and then incubated with anti-V5-FITC antibody (1:1000 dilution) for 15 min at room temperature in the dark. Following two successive washes, both groups of cells were subjected to flow cytometry in an EPICS XL flow cytometer (Beckman Coulter) [8].

Measurement of intracellular cAMP. In Hanks' buffer containing 20 mM Hepes and 0.2% bovine serum albumin, transfected cells were exposed to the indicated concentrations of hAM for 15 min at 37 °C in the presence of 0.5 mM 3-isobutyl-1-methylxanthine (Sigma). The reactions were terminated by addition of lysis buffer (GE Healthcare), after which the cAMP content was determined using a commercial enzyme immunoassay kit according to the manufacturer's instructions (GE Healthcare) for the non-acetylation protocol.

Statistical analysis. Results are expressed as means ± SEM of at least three independent experiments. Differences between two groups were evaluated using Student's *t*-tests; differences among multiple groups were evaluated using one-way analysis of variance followed by Scheffe's tests. Values of $p < 0.05$ were considered significant.

Results

Characterization of VPAC2 overexpressed in HEK-293 cells with or without RAMPs

When transfected into HEK-293 cells, VPAC2 mediated marked, concentration-dependent increases in cAMP in response to VIP (EC_{50} = 0.64 ± 0.03 nM) (Fig. 1A). But neither AM nor CGRP elicited cAMP production in VPAC2 transfectants (Fig. 1A), which was comparable to that seen in cells transfected with CRLR [6,11] or RAMP2 [11]. These findings confirm that our HEK-293 cells lack both functional RAMPs and CRLR, that the VPAC2 is unable to function as an AM or CGRP receptor. In the present study, therefore, we used FACS analysis of HEK-293 cells to evaluate the interaction between RAMP and VPAC2 or CRLR/VPAC2 chimeras.

We initially tested whether VPAC2 interacts with any of the three RAMPs. Surface binding of anti-V5-FITC antibody was within the 2% limit of resolution when cells were transfected with empty vector (*Mock*). When expressed alone FITC-labeled V5-CRLR was detected in ~30% of cells (Fig. 3). When co-expressed with wild-type RAMP1, -2 or -3, the surface expression frequency was significantly increased (Fig. 3). By contrast, the surface expression of V5-VPAC2 (42.2%) was not increased by co-transfection with RAMP1, -2 or -3 (39.2%, 39.8% and 38.8%, respectively) (not shown).

Subsequent comparison of the changes in the frequency of surface expression of V5-RAMP1, -2 and -3 co-transfected with wild-type CRLR or VPAC2 (Figs. 1A–C) revealed that surface expression of V5-RAMP1 and -2 was markedly increased by co-transfection of CRLR but not VPAC2. In contrast to V5-RAMP1 and -2, V5-RAMP3 appeared at the surface of 19.0% of cells when the protein was expressed alone, provably due to its self-transport to the cell surface [12] or its interaction with other endogenous GPCRs [2,4]. Still, although the cell surface expression of V5-RAMP3 was further increased by co-transfection of CRLR, it was unaffected by VPAC2. Thus the observed pattern of cell-surface expression is consistent with there being no interaction between VPAC2 and any of the three RAMPs.

FACS analysis of the trafficking interaction between RAMP and CRLR/VPAC2 chimeras

Because there are no interactions between VPAC2 and RAMPs, we constructed a set of nine chimeric CRLR/VPAC2 receptors (Fig. 2A) to evaluate the trafficking interactions between specific CRLR domains and each of RAMPs. These chimeras were then transiently co-transfected with each RAMP into HEK-293 cells, and their interaction was characterized using flow cytometry.

We initially analyzed the total expression of each of the V5-tagged chimera in permeabilized cells when transfected alone

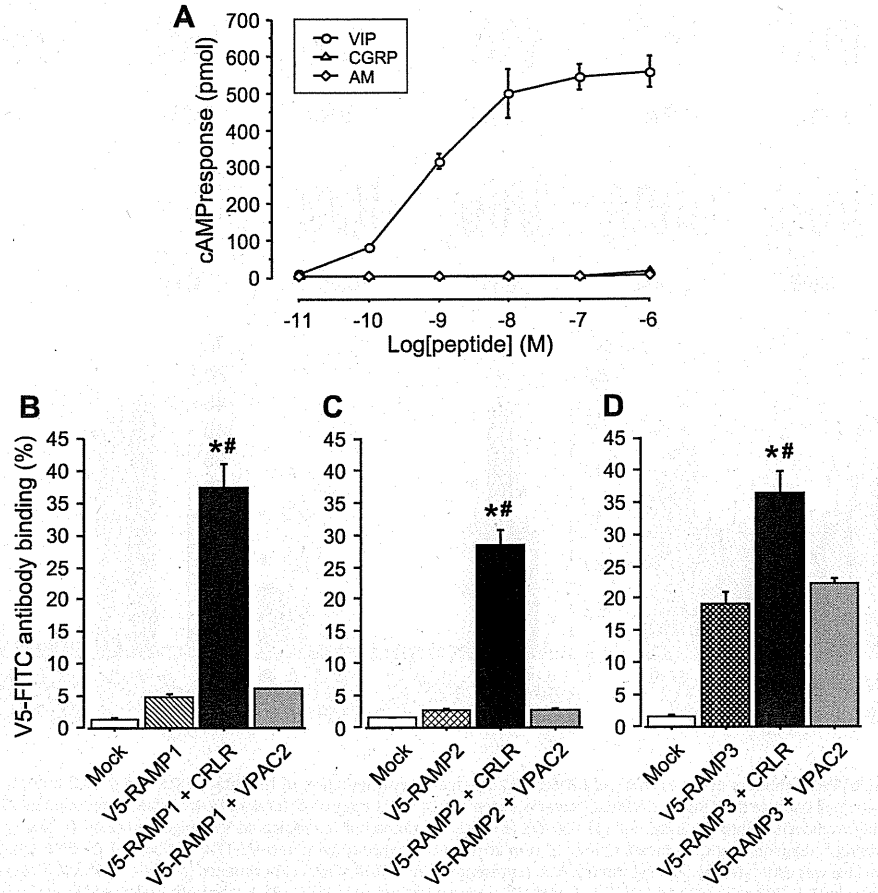

Fig. 1. Characterization of VPAC2 overexpressed in HEK-293 cells. (A) Agonist-evoked cAMP production in HEK-293 cells expressing VPAC2 alone. Cells were transiently transfected with VPAC2, after which they were stimulated with the indicated concentrations of VIP, CGRP or AM for 15 min at 37 °C and then lysed. The resultant lysates were analyzed for cAMP content. Bars represent means ± SEM of three experiments. FACS analysis of the cell surface expression of V5-RAMP1 (B), V5-RAMP2 (C) and V5-RAMP3 (D) following transfection into HEK-293 cells, with or without CRLR or VPAC2. Forty-eight hours after transfection, cells were incubated for 1 h at 4 °C with monoclonal anti-V5-FITC antibody; mock incubation with the antibody served as the control. FITC-labeled V5-CRLR and V5-VPAC2 expressed at the cell surface were separately estimated by flow cytometry. Bars represent means ± SEM of three to four experiments. $^{*}p < 0.0005$ vs. Mock; $^{\#}p < 0.001$ vs. the corresponding V5-RAMP alone.

(Fig. 2B). FITC-labeled CRLR was detected in 53.1% of cells, and similar results were observed in VPAC2 transfectants. Among the nine chimeras tested, full expression of CH1, -8 and -9 was detected in 38–45% of cells. Transfection of the remaining six chimeras led to their full expression in 25–31% of cells. Thus the transfection efficacies of the chimeras did not significantly differ from that of CRLR.

We next analyzed the cell surface expression of the V5-tagged constructs in non-permeabilized HEK-293 cells when expressed alone (Fig. 2C). FITC-labeled CRLR was detected in 27.4% of cells, despite of the absence of RAMPs, which is consistent with earlier observations [11,13]. V5-VPAC2 transfection led to its strong surface expression in 52.5% of cells. Surface expression of three chimeras, CH1, -8 and -9, was detected in 14–32% of cells. The remaining six chimeras appeared at the surface of only 2.0–2.6% of cells.

Although COS-7 cells express no functional RAMPs [3,14], there have been several reports showing that tagged CRLR is highly expressed at the cell surface when transfected alone [13,15]. As shown in Fig. 2D, V5-CRLR appeared at the surface of 45.2% of COS-7 cells, which was a higher frequency than in HEK-293 cells (Fig. 2C). Similar differences in surface receptor expression between these two cell types were also observed when the cells were transfected with chimeras CH1 and CH9. The cell surface expression of the other chimeras was similar to that seen in HEK-293 cells.

We also examined the effects of co-transfecting each wild-type RAMP on the surface expression of V5-tagged chimeras in HEK-293 cells (Fig. 3). Surprisingly, co-transfection of RAMP1, -2 or -3 led to markedly greater increases in surface delivery of two chimeras, CH6 and CH7, than was seen with V5-CRLR. On the other hand, co-transfection of RAMPs had no substantial effect on the cell-surface expression of the other chimers.

We next measured V5-RAMP translocation to the cell surface as a marker of RAMP–receptor interaction (Fig. 4). The surface expression of V5-RAMP1, -2 and -3 was markedly increased by co-transfection of two chimeras, CH7 and CH8. By contrast, co-transfection of CH2, -3, -4, -5 or -9 did not increase translocation of the three RAMPs. Co-transfection of CH1 significantly increased surface expression frequency of V5-RAMP1 to 29.4%, which is ~75% of that seen with CRLR. Similarly, CH1 increased the frequency of V5-RAMP3 surface expression to a level equal to that seen with CRLR, whereas CH1 did not significantly increase cell-surface delivery of V5-RAMP2. Co-transfection of CH6 markedly increased the frequency of surface expression of V5-RAMP1 and -3 to a level comparable to that seen with CRLR, while increases in surface expression of V5-RAMP2 mediated by CH6 were about half of those seen with CRLR.

Discussion

That surface expression of V5-CRLR in HEK-293 cells was significantly increased by co-transfection of each of the three RAMPs is

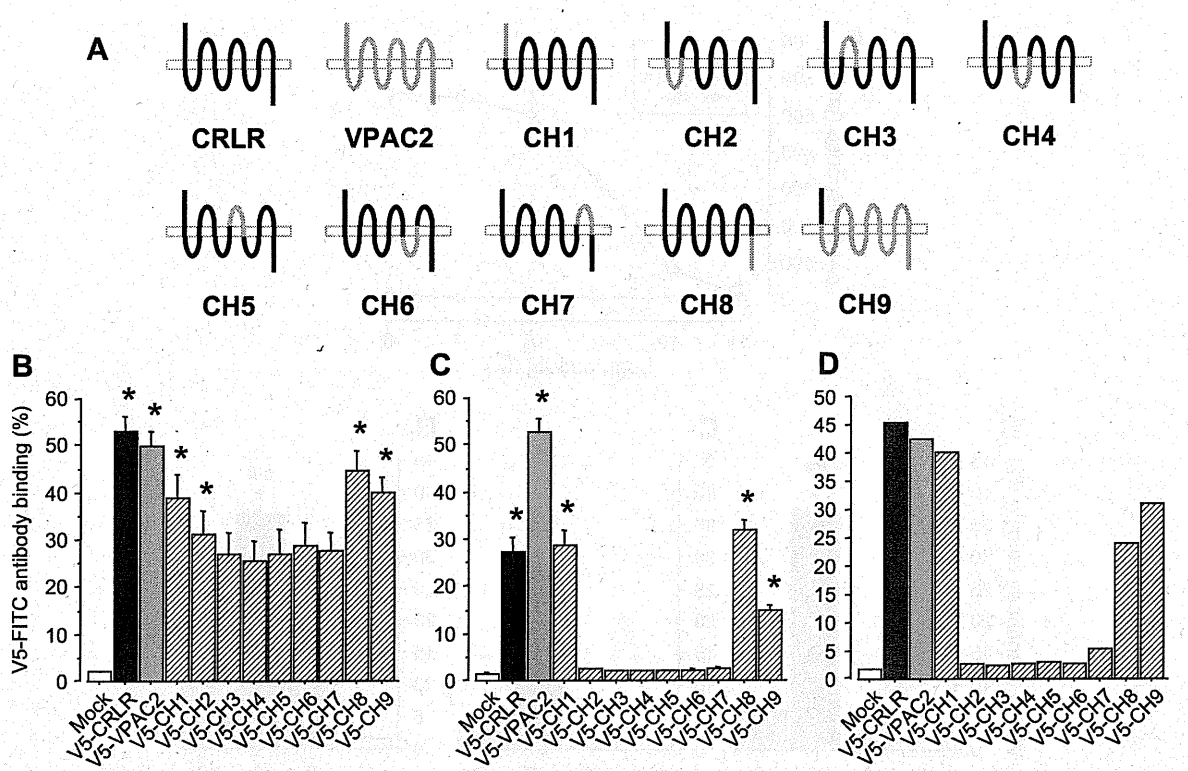

Fig. 2. Characterization of CRLR/VPAC2 chimers in the absence of RAMPs. (A) Schematic representation of the intact CRLR and VPAC2 and the nine CRLR/VPAC2 chimeras (CH1–CH9). Bold black and gray lines indicate the CRLR and VPAC2 domains, respectively. FACS analysis of total and cell surface expression of V5-CRLR, V5-VPAC2 or the V5-CRLR/VPAC2 chimeras following transfection into the indicated cells (B–D). (B) Total expression of the indicated V5-tagged proteins. Following transient transfection, cells were permeabilized with IntraPrep™ reagents and then incubated for 15 min at room temperature with anti-V5-FITC antibody. Each FITC-labeled protein expressed in the cytoplasm and/or at the cell surface was estimated by flow cytometry. Bars represent means ± SEM of four experiments. $^{*}p < 0.04$ vs. Mock. (C and D) Cell surface expression of the indicated V5-tagged proteins in HEK-293 cells (C) and COS-7 cells (D). Cells were analyzed as in Fig. 1. Bars represent means ± SEM of four experiments for (C) and two experiments for (D). $^{*}p < 0.01$ vs. Mock.

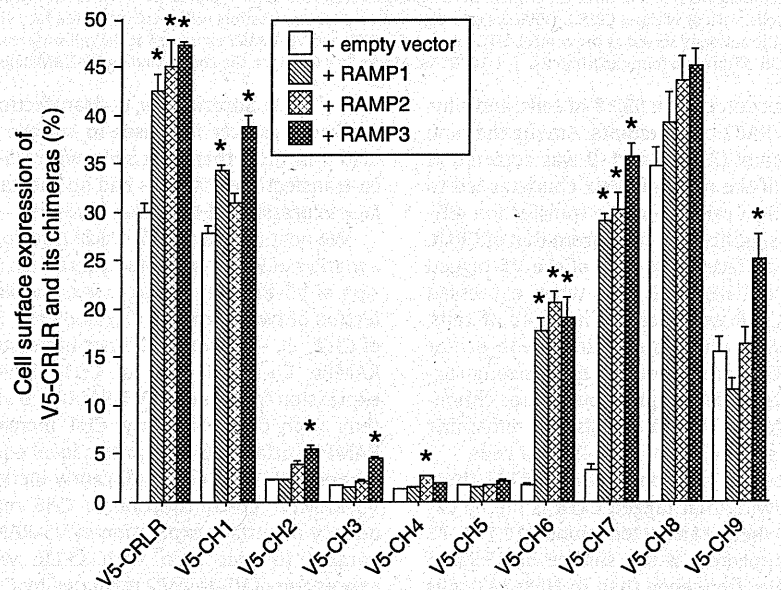

Fig. 3. FACS analysis of cell surface expression of V5-CRLR and the V5-CRLR/VPAC2 chimeras following transfection into HEK-293 cells, with or without RAMP1, -2 or -3. After transfection, cells were analyzed as in Fig. 1. Bars represent means ± SEM of three experiments. $^{*}p < 0.05$ vs. the corresponding V5-CRLR alone or V5-CRLR/VPAC2 chimera alone.

indicative of the trafficking interactions between CRLR and RAMPs (Fig. 3). Each of the RAMPs can also associate with the CT receptor, thereby forming three functional amylin receptors [2,14]. But surface expression of the CT receptor is not increased by co-transfec-